JOURNAL OF Materials Feature Article CHEMISTRY

Structural order in conjugated oligothiophenes and its implications on opto-electronic devices

Denis Fichou*

Laboratoire des Matériaux Moléculaires, C.N.R.S., 2 rue Henry Dunant, 94320 Thiais, France. E-mail: fichou@glvt-cnrs.fr

Received 18th October 1999, Accepted 6th December 1999

Over the last ten years, conjugated oligothiophenes have emerged as one of the largest families of organic semiconductors with potential applications in electronics devices. Thin film transistors (TFTs), photovoltaic solar cells, light-emitting diodes (LEDs), light modulators, photochromic switches and laser microcavities are some examples of devices that have been fabricated with oligothiophenes as the active materials. The key advantage of well-defined oligomers over their parent polymers is the high degree of molecular and crystalline ordering they can achieve. Polycrystalline and highly oriented thin films can be easily prepared from solution or by vacuum deposition. In many cases it has even been possible to grow single crystals and elucidate their X-ray structure. The aim of this review is to describe the structure of oligothiophene crystals and thin films and to explore its implications on the performances of various electronic devices.

1 Introduction

The recent and spectacular development of conjugated oligothiophenes is essentially related to their use as active materials for electronic device applications.[1] As long ago as 1974, an initial article by H. Kuhn *et al.*[2] described photocurrent measurements on Langmuir–Blodgett films of α-quinquethiophene (α-5T). In the mid-1980's, conjugated all-α-linked oligothiophenes (α-*n*T, with n = number of thiophene rings in the oligomeric sequence, see Scheme 1) were used as model compounds and starting monomers for the preparation of electrically conducting polythiophenes.[3–5] Many bi- and terthiophene derivatives also exhibit biological activities such as phototoxicity[6] or antibiotic and antiviral properties in the presence of UVA light.[7,8]

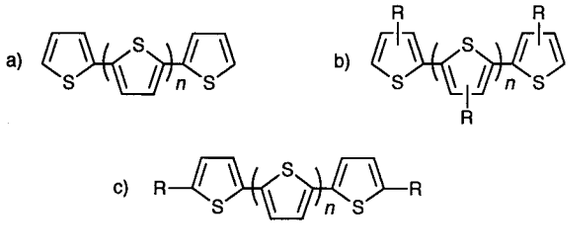

Scheme 1

The true starting point of the contemporary generation of α-oligothiophenes is the discovery, in 1988 by the CNRS group in Thiais, of the charge transport properties of α-sexithiophene (α-6T).[9,10] A year later, evaporated thin films of α-6T were used as the p-type semiconductor of an organic field-effect transistor (FET).[11,12] The mobilities of majority carriers measured in these devices were in the range $\mu = 10^{-3}$ to 10^{-4} cm^2 V s^{-1}, *i.e.* one to two orders of magnitude higher than those of PT-based FETs[13,14] but still substantially lower than those of conventional a-SiH based MISFETs.[15] In 1990, well before the first polymer light-emitting diode on a flexible substrate, it was demonstrated that an *all-organic* α-6T FET could be fabricated on a flexible polymer substrate, thus opening the era of "plastic electronics".[16]

Since then, emphasis has been put on the electronic structure[17–20] and charge transport properties[21–24] of semiconducting α-*n*T thin films. These studies are essentially motivated by their implications on charge transport in thin film transistors (TFTs).[25] In particular, it has been demonstrated that α-6T-based TFTs show an improved carrier mobility when long range molecular ordering is achieved.[26] The highest mobilities ($\mu_{FE} = 0.04$ cm^2 V^{-1} s^{-1}) are obtained in TFT devices using highly oriented thin films and are close to that measured on α-6T single crystals ($\mu_{FE} = 0.16$ cm^2 V^{-1} s^{-1}).[27] This shows that charge transport between source and drain of a TFT occurs essentially through molecular channels of α-6T molecules oriented perpendicular to the substrate and having the herringbone arrangement found in the single crystal.

Great progress has thus been accomplished in the understanding and fabrication of organic FETs resulting in higher mobilities, reduced size, and easy processability.[28] Finally, oligothiophenes have also been used in devices such as light-emitting diodes,[29,30] spatial light modulators,[31] electro-optical modulators[32–34] and photovoltaic cells.[35–38] The main characteristics of these devices have been recently summarized by Granström *et al.*[39]

The aim of this review is to summarize the structural aspects of long oligothiophenes in the solid state (α-4T and higher homologs) and to explore their implications on the operation and performances of some electronic devices. Most short oligothiophenes (α-2T, α-3T and derivatives) do not possess the appropriate electronic properties required for device applications and will not be addressed in this review. Polythiophene (PT) and its substituted derivatives will be briefly considered here as examples of disordered parent materials. An exhaustive review of thiophene-based electronic devices has been published elsewhere.[1]

2 Structural data of oligothiophenes

2.1 Single crystals

2.1.1 Overview. The crystal structure of most α-oligothiophenes has been investigated recently, in contrast to oligophenylenes for which structural data have been known for two decades.[40–43] With the exception of α-septithiophene (α-7T), single crystals of non-substituted α-oligothiophenes have been grown and characterized up to the octamer α-8T. The structures of various end- and side-substituted α-*n*T derivatives have also been determined, for example 2,5‴-dimethylquaterthiophene[44] or 3′,3‴′,4′,4‴′-tetrabutylsexithiophene.[45] Beside experimental studies, computational procedures have

been used in some cases to confirm, refine or predict the crystal structure of α-*n*Ts. One important contribution of theoretical simulations is to identify the origin of crystal packing in terms of intra- and intermolecular forces.

In the crystalline form, all non-substituted oligothiophenes are quasi-planar, *i.e.* the inter-ring torsion angle is $<1^\circ$. One exception is α-3T for which a 6–9° deviation from planarity has been reported.[46] This coplanarity in the solid state compensates for the non-rigid conformation of α-*n*Ts in the gas phase and in solution and is responsible for their high π-delocalisation. Introduction of one or several side substituents on the β-positions of the thiophene rings induces the loss of planarity and consequently affects transport properties.

In 1991, Gavezzotti and Filippini calculated the crystal packing of α-*n*T oligomers up to α-6T and demonstrated the general trend of these molecules to pack in a parallel fashion with angles of 40–60° between molecular planes of side-by-side molecules and S···S contacts between 3.6 and 3.9 Å.[47] This predicted "herringbone" (HB) arrangement, which is typical of many aromatic hydrocarbons such as *para*-oligophenylenes and acenes, was later experimentally confirmed. The origin of the HB packing mode is mainly due to the repulsion between π-orbitals of neighbouring molecules. X-Ray studies on polycrystalline thin films of α-*n*Ts have also revealed a HB packing.[48–52] This particular molecular arrangement will probably reduce the transport properties in the direction normal to the long molecular axis. Two ways can be envisaged to force molecules to escape the HB packing and adopt a π-stack (or sandwich-type) structure with face-to-face molecules: substitution and doping. Substitution, or chemical modification of the molecule by appropriate substituents, may create strong intermolecular interactions (through for example H-bonds) and overcome the π–π repulsion. Alternatively, chemical or electrochemical oxidative doping of oligothiophenes produces their radical cation forms whose fully coplanar quinoid structure may crystallize in a π-stack mode.

All non-substituted α-*n*Ts crystallize in the monoclinic system with a $P2_1$ space group ($P2_1/a$, $P2_1/c$ or $P2_1/n$ depending on the oligomer length). The number of molecules per unit cell is $Z=2$ for α-2T[53–55] and $Z=8$ for α-3T[46] while it is $Z=4$ for longer oligomers α-4T,[56,57] α-5T,[48,58] α-6T[59] and α-8T.[60] Although for α-3T, α-5T and α-8T single crystals a unique crystallographic phase has been observed, two different structures have been identified for both α-4T[56,57] and α-6T.[51,61] In these two cases, one form packs with $Z=2$ while the other one adopts a $Z=4$ structure. Note that polymorphism has also been observed in the *para*-oligophenylene series.[43] The main crystallographic data of non-substituted oligothiophenes are gathered in Table 1.

The determination of the structure of PTs is limited by their inherent low crystallinity.[62] Nevertheless, two stable conformations, a nearly planar all-*trans* rod and a all-*cis* helical or coil geometries, can be predicted from theoretical calculations for polythiophene.[63]

2.1.2 Long oligothiophenes. *α-Quaterthiophene (α-4T) and derivatives.* The X-ray structure of α-4T (Scheme 2) single crystals grown from the vapor phase has been solved simultaneously by two groups.[56,57] Nevertheless, data had been previously predicted on the basis of calculations by Gavezzotti and Filipini[47] and further refined by Porzio *et al.* from X-ray powder diffraction using the Rietveld full-profile analysis.[48,58]

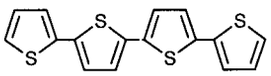

Scheme 2

The unit cell is monoclinic with a $P2_1/a$ space group and the α-4T molecules are planar. It is worth noting that crystals grown from the vapor phase are in the form of thin platelets while microcrystals obtained from solution are reported to be needles.[48] The number of molecules per unit cell is $Z=4$ although the minimization of the packing potential energy led Gavezzotti and Filippini to predict a $Z=2$ structure.[47] This choice was dictated by a principle of organic crystallography according to which organic molecules tend to make their centre of symmetry coincide with a crystal centre of symmetry.

From the comparison between the above results and those simultaneously obtained by Antolini *et al.*[56] and Siegrist *et al.*,[57] it appears clearly that α-4T crystallizes in two slightly different structures depending on the crystal growth conditions. Such polymorphism has been observed previously on α-6T crystals grown either from the melt or by sublimation (*vide infra*). The two structures differ by the number of molecules in the unit cell ($Z=4$ or $Z=2$). The experimental herringbone angle, *i.e.* the angle between mean planes of adjacent molecules, has been found to be of the order of 55°[56,57] for α-4T grown from the vapor phase while a substantially greater value (70°) was found from X-ray diffraction data obtained with polycrystalline powders.[58] But the most striking difference is that the two polymorphs have different packing modes, neighbouring molecules being more or less staggered relative to each other (Fig. 1).[57]

Ferro *et al.* recently used a molecular mechanics computational procedure to refine and understand the crystal structure of α-4T, α-6T and PT.[64] For both oligomers, calculations maintain the essential features of the original structure proposed by Porzio *et al.*[48] Both α-4T and α-6T have a molecular centre of inversion which does not act on the crystal packing.

Table 1 Comparative experimental structural data of non-substituted oligothiophene single crystals

	α-2T	α-3T	α-4T/LT	α-4T/HT	α-5T	α-6T/LT	α-6T/HT	α-8T
Reference	54	46	48	56,57	48	59	61	60
System	Monoclinic	Monoclinic	Monoclinic	Monoclinic	Monoclinic	Monoclinic	Monoclinic	Monoclinic
Space group	$P2_1/c$	$P2_1/c$	$P2_1/a$	$P2_1/a$	$P2_1/a$	$P2_1/n$	$P2_1/a$	$P2_1/a$
Z	2	8	4	2	4	4	2	4
a/Å	7.873	15.225	30.52	8.936	39.00	44.71	9.14	58.92
b/Å	5.771	5.635	7.86	5.750	7.77	7.85	5.68	7.84
c/Å	8.813	25.848	6.09	14.341	6.00	6.03	20.67	6.00
β/deg	107.07	98.15	91.8	97.22	97.7	90.8	97.78	90.3
τ^a/deg			72	55.67	65	66	55	65
ϕ^b/deg				31.5		23.5	41.5	24
D^c/Mg m^{-3}	1.44	1.503	1.50	1.501	1.55	1.553	1.55	1.578
Volume/Å^3	382.8	2195.2		731.1		2116.5	1064.2	2773.0

[a] τ, herringbone angle. [b] ϕ, tilt angle of the long molecular axis with a. [c] D, calculated density.

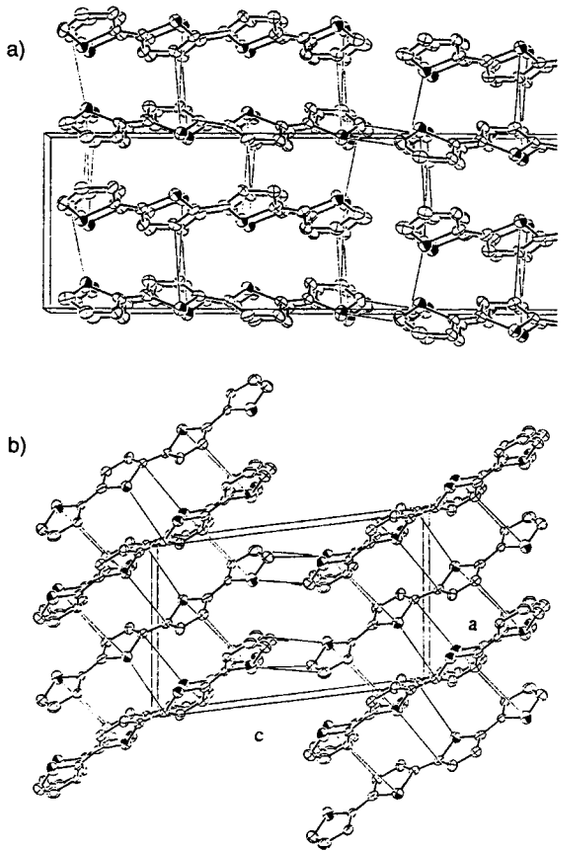

Fig. 1 Packing diagrams of the two α-quaterthiophene (α-4T) polymorphs. Low temperature α-4T/LT (a) and high temperature α-4T/HT (b). Reproduced with permission from ref. 57.

α,α′-Dimethylquaterthiophene [α-4T(α-Me)$_2$]. The end-substitution of oligothiophenes by alkyl groups is an efficient method for preventing chemical reactivity of these sites. In addition to enhanced chemical stability, end-substitution does not induce inter-ring torsion (as often does side-substitution) thus retaining high π-conjugation and electroactivity. Hotta and Waragai have applied this strategy to α-4T and investigated the crystal structure of α-4T(α-Me)$_2$ (Scheme 3) in its neutral form[25,44] while its doped form was studied by Matsuura *et al.*[65]

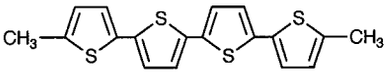

Scheme 3

In contrast to non-substituted α-oligothiophenes, crystals of neutral α-4T(α-Me)$_2$ are orthorhombic with a *Pbca* space group and $Z=4$. The molecules are almost coplanar, the two outer rings being slightly bent according to the mean plane of the two inner ones (maximum deviation is *ca.* 0.16 Å for C_8). Although packed in the HB mode with an angle of about 59° between adjacent molecular planes, the molecules are aligned in an unusual zigzag fashion, the molecular long axis being at an angle of 26° with the *c* axis.

Hotta and Waragai have shown that α-4T(α-Me)$_2$ crystals can also be grown in their doped form using acceptors like iodine, $NOBF_4$, $NOPF_6$ or $TCNQF_4$.[44] X-Ray analysis of these doped crystals shows a layered structure similar to that of the neutral compound although the profile of fine needles of the $TCNQF_4$-doped crystal is considerably more complicated than that of the iodine-doped one. The authors measured electrical conductivities of 3.4×10^{-5} S cm^{-1} along the *c*-axis, *i.e.* vertical to the crystal plane, and 1.2×10^{-1} S cm^{-1} and 2.9×10^{-2} S cm^{-1} for the directions longitudinal and transversal along the crystal plane respectively. The latter directions, however, do not coincide neither with the *a*- or *b*-axis of the molecules. This also argues in favor of a preferred charge transport along the π-stacks rather than along the molecular axis. Nevertheless, Hotta and Waragai explain this as the effect of the iodine anions which are located between the ends of the molecules, thus preventing charge carriers from hopping from one site to the next one. The electrical conductivity within the blade plane has also been measured for various dopants,[44] *i.e.* I_2 (1.0×10^{-1} S cm^{-1}), $NOBF_4$ (4.4×10^{-2} S cm^{-1}) and $NOPF_6$ (2.1×10^{-2} S cm^{-1}), showing that α-4T(α-Me)$_2$ is a quasi-2D conductor in which transport essentially occurs through face-to-face molecular arrays.

4,4′,3″,4″-Tetramethylquaterthiophene [α-4T(β-Me)$_4$]. One of the most widely investigated conducting polythiophenes is poly(3-methylthiophene) P3MeT. As stated above, introduction of a substituent on the thiophene rings may induce conformational twist along the polymer chain and consequently decrease its mean conjugation length. An elegant way to evaluate precisely the influence of substitution on the P3MeT polymer structure is to synthesize a regioselective oligomer.

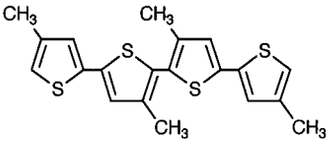

Scheme 4

The crystal structure of the model compound α-4T(β-Me)$_4$ (Scheme 4) has been investigated in comparison with its conformation in solution.[66,67] Crystals of α-4T(β-Me)$_4$ are monoclinic with a $P2_1c$ space group and $Z=2$. The molecules are stacked in parallel layers along the *a* axis similarly to unsubstituted oligothiophenes. The strong steric interactions introduced by the four methyl groups on the β-carbons break neither the coplanarity of the α-4T(β-Me)$_4$ molecule in the crystal nor the all-*trans* conformation as it does in solution (*cis–trans–cis* conformation with an angle of 40° between the planes of the two internal rings). Nevertheless, methyl-substitution induces bond length and angle deformations in the solid state. Barbarella *et al.* attribute this effect more to the ability of the α-4T(β-Me)$_4$ molecule to retain maximum π-conjugation through coplanarity rather than crystal packing forces.

3,3′,4″,3‴-tetrakis(methylsulfanyl)-2,2′ : 5′,2″:5″,2‴-quaterthiophene. Another example of polymorphism is reported on 3,3′,4″,3‴-tetrakis(methylsulfanyl)-2,2′ : 5′,2″ : 5″,2‴-quaterthiophene (noted α-4T(β-SMe)$_4$, Scheme 5).[68,69] This molecule crystallizes in two distinct forms under the same experimental conditions. This phemomenon, known as *conformational polymorphism*, in which a molecule adopts different conformations in crystal polymorphs, was elucidated by Bernstein and Hagler twenty years ago.[70] A recent review by Dunitz and

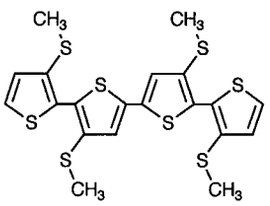

Scheme 5

Table 2 Comparative crystal data of α-4T derivatives

	α-4T/LT[b]	α-4T/HT[b]	α-4T(α-Me)$_2$	4T(β-Me)$_4$	4T(β-SMe)$_4$	4T(β-SMe)$_4$
Reference	48	56,57	44	66	68	69
System	Monoclinic	Monoclinic	Orthorhombic	Monoclinic	Triclinic	Monoclinic
Space group	$P2_1/a$	$P2_1/a$	*Pbca*	$P2_1/c$	$P1$	$P2_1/c$
Z	4	2	4	2	1	2
a/Å	30.52	8.936	7.707	7.734	7.567	12.345
b/Å	7.86	5.750	5.941	5.729	7.601	7.565
c/Å	6.09	14.341	36.031	8.933	11.193	12.784
α/deg					93.99	
β/deg	91.8	97.22	90	106.72	100.88	97.14
γ/deg					116.75	
D_c/Mg m^{-3} [a]	1.50	1.501	1.444	1.457	1.538	1.443
Volume/Å^3	1470.5	731.1	1649.8	379.0	555.80	1184.7

[a] D_c, calculated density. [b] LT, low-temperature polymorph. HT, high temperature polymorph.

Bernstein on "disappearing polymorphs" illustrates the difficulty in obtaining a particular conformer under controlled and reproducible conditions.[71]

The crystal structures of the triclinic and monoclinic forms of α-4T(β-SMe)$_4$ are given in Table 2. In the orange triclinic crystal, the inner thiophene rings are coplanar while the two outer ones are twisted by 27.4° according to the plane of the central rings.[68] But the most interesting feature is that the triclinic form has a sandwich-type molecular arrangement instead of the usual herringbone packing. Barbarella *et al.* tentatively attribute this *quasi-π-stack* to the partial loss of coplanarity of the molecule. In the yellow monoclinic form the two outer rings are even more twisted (55.0°) resulting in a substantial π-delocalization decrease and hence a yellow color.

α-Quinquethiophene (α-5T) and derivatives. The structure of α-5T (Scheme 6) single crystals has not been elucidated yet and the only studies have been performed on sublimed powders by Porzio *et al.*[48] Considering that α-5T is isomorphous with α-4T and α-6T, these authors found that the dimensions of the α-5T unit cell are intermediate between those of α-4T and α-6T (see Table 1) but mention that this was not expected due to the odd number of thiophene rings which induces a different internal symmetry.

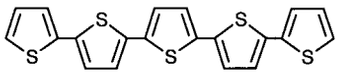

Scheme 6

3″,4″-Dibutyl-α-quinquethiophene [α-5T(β-Bu)$_2$]. The X-ray crystal structure of α-5T(β-Bu)$_2$ (Scheme 7) has been recently investigated by Liao *et al.* together with that of a β-tetra-alkylated sexithiophene derivative.[45] In both cases, the β-alkyl chains induce structural and conformational deviations. The α-5T(β-Bu)$_2$ unit cell ($Z=8$) contains four independent molecules, one of them having its two terminal thiophene rings in the *syn* conformation similarly to the yellow monoclinic form of the α-4T(β-SMe)$_4$ crystal.[86] The *syn* conformation of this oligomer is reminiscent of the coil geometry claimed for polythiophene.

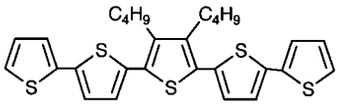

Scheme 7

α-Sexithiophene (α-6T) and derivatives. The first crystal structure of α-6T (Scheme 8) was reported by Porzio *et al.* using the Rietveld full-profile analysis on polycrystalline powder samples.[48] In agreement with the theoretical predictions,[47] these authors found a $P2_1/a$ space group with four molecules in the unit cell ($Z=4$). Note that beside solid state crystals, a nematic liquid crystal mesophase has been observed with α-6T by Taliani *et al.*[72] This phase appears at 312 °C as measured by differential scanning calorimetry. Cooling the samples below the melting point leads to a freezing of the α-6T nematic phase. The formation of an α-6T mesophase above 305 °C has also been observed by Destri *et al.* but could not be assigned to either a nematic or smectic phase.[73]

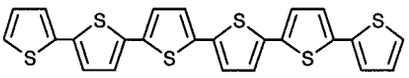

Scheme 8

Macroscopic α-6T crystals with millimetre-scale transverse dimensions were obtained in 1995 simultaneously by Siegrist *et al.* from the melt at high temperature (α-6T/HT)[61] and by Horowitz *et al.* using a sublimation technique (α-6T/LT)[59] adapted from that of Lipsett.[74] By refining the sublimation technique, we recently were able to produce α-6T crystals of exceptional size and quality. Fig. 2 shows a α-6T/LT crystal 8 mm in diameter (thickness of 5–10 microns only) grown by slow sublimation at 160 °C over 72 hours. As observed under polarized light, most of its area appears defect-free. The highly disordered aggregate on the right part of the photograph is the matrix root of the sample. Note that Schön *et al.* have also produced large α-6T/HT crystals of high quality by using a higher growth temperature (280–320 °C).[75] These authors report a record mobility of $\mu_{SCLC}=0.46$ cm^2 V^{-1} s^{-1}

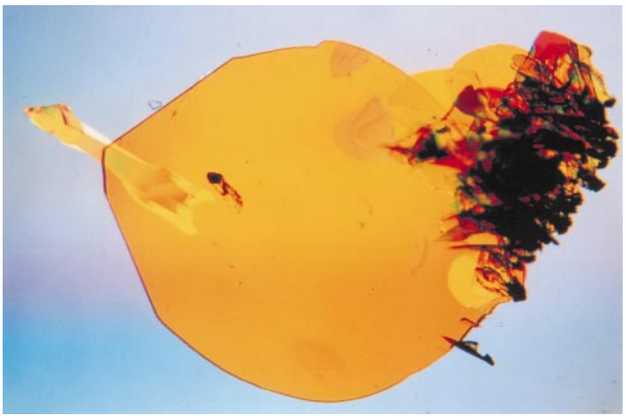

Fig. 2 Optical micrograph of a α-6T single crystal (length = 8 mm; thickness = a few μm). The disordered aggregate on the right is the matrice root of the sample. Note the high quality of this crystal, at the exception of the small twin crystal on left.

(SCLC = space charge limited current) for the HT form along the crystallographic direction with the best orbital overlap between molecules. Schön *et al.* also report a mobility of the HT polymorph which is twice that of the LT form ($\mu_{SCLC} = 0.21\ cm^2\ V^{-1}\ s^{-1}$).

The two kinds of α-6T crystals (LT and HT) have two different crystal structures.[61,76] While $Z = 4$ is found in crystals grown from the vapor phase, crystals grown from the melt (the so-called "high temperature polymorph" α-6T/HT) are characterized by $Z = 2$ (see Table 1). Both structures are monoclinic with flat molecules in the usual herringbone packing but they slightly differ in the position and orientation of the molecules in the unit cell (Fig. 3). A similar polymorphism is observed with α-4T depending on the sample quality, *i.e.* single crystals grown by sublimation[56,57] or polycrystalline powder.[58] The structure of α-6T crystals obtained from the vapor phase is very similar to that of α-8T ones grown by the same technique.[60]

Alkylated-α-sexithiophenes. Before the elucidation of the crystal structure of non-substituted α-6T, a few alkylated α-6T derivatives have been studied. In particular, Herrema *et al.*[77] synthesized two stereoregular dialkyl α-6T and investigated their X-ray structure. Both 4′,3‴″-dibutylsexithiophene (Scheme 9) and bis(trimethylsilyl)dioctylsexithiophene (Scheme 10) crystals grown from solution crystallize with the monoclinic system in respectively the $C2/c$ and $P2_1/n$ space group. In spite of the bulky substituents, the molecules are almost planar with the antiparallel conformation.

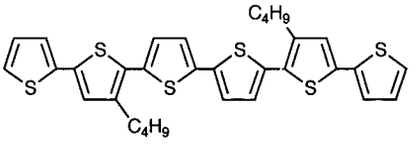

Scheme 9

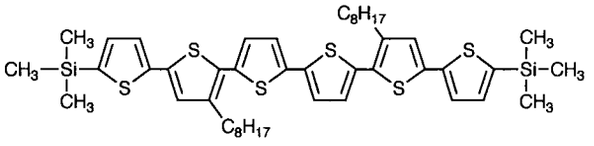

Scheme 10

These results support the idea that the *syn* or *anti* conformations are essentially determined by packing forces at the detriment of intramolecular forces. This is nicely illustrated by the results obtained by Liao *et al.* on 3″,4″-dibutylquinquethiophene and 3′,3‴″,4′,4‴″-tetrabutylsexithiophene (Scheme 11).[45] In the unit cell ($Z = 4$) of the latter, three molecules have an all-*anti* conformation while in the fourth molecule the external rings have a *syn* conformation relative to their neighbor. Furthermore, the external rings substantially deviate from the coplanarity of the molecule whatever their *syn* or *anti* conformation.

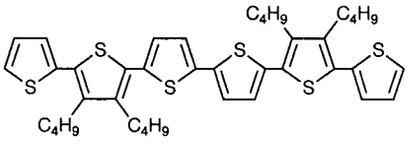

Scheme 11

End-substituted sexithiophenes. Blocking the two end-positions of the oligomer may in some cases increase crystal ordering and consequently transport properties. Higher mobilities have been recorded when the terminal H of 6T are

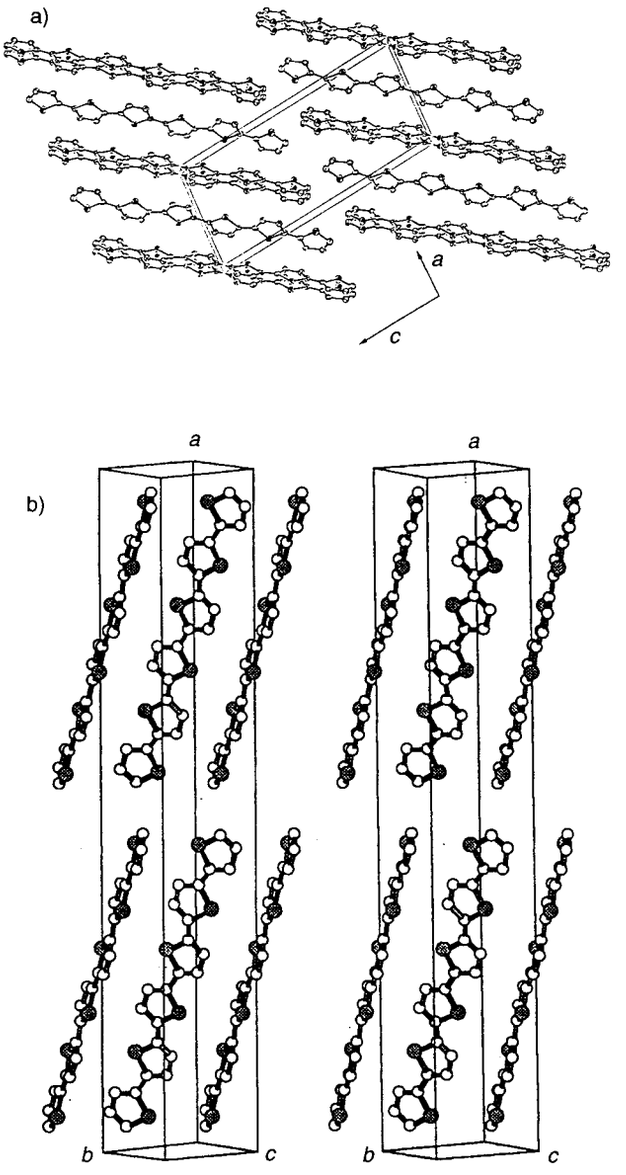

Fig. 3 Crystal structures of the two α-6T polymorphs obtained (a) from the melt at high temperature α-6T/HT (reproduced with permission from ref. 61) and (b) from the vapor phase at relatively low temperature α-6T/LT.[59] (Reprinted with permission from *Chem. Mater.*, 1995, **7**, 1337. Copyright 1995 American Chemical Society).

replaced by *n*-hexyl groups.[78] In contrast, end-substitution by silyl groups results in very low field-effect mobilities in the range 10^{-4} to $10^{-7}\ cm^2\ V^{-1}\ s^{-1}$.[79] α,ω-Bis(triisopropylsilyl)-sexithiophene (Scheme 12) crystallizes from a heptane solution as leaf-shaped brownish crystals in the unusual triclinic system with only one molecule per unit cell ($Z = 1$).[80] The most striking feature is that, although the molecules have an antiparallel conformation with no substituent on the β-positions, all rings are strongly twisted around the central axis. The main crystal data of sexithiophene derivatives are gathered in Table 3.

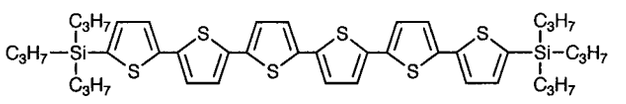

Scheme 12

Barclay *et al.* synthetized a series of oligothiophenes symmetrically substituted by two CN groups in terminal α-positions.[81] All compounds are planar and linked into ribbon-like arrays by intermolecular CN···H contacts.

Table 3 Comparative crystal data of α-6T derivatives

	α-6T	α-6T/HT	α-6T(β-Bu)$_2$	α-6T(α-SiMe$_3$)$_2$(β-Oct)$_2$	α-6T(β-Bu)$_4$	α-6T(α-SiPr$_3$)$_2$
Reference	59	61		79	45	80
System	Monoclinic	(Monoclinic)	Monoclinic	Monoclinic	(Monoclinic)	Triclinic
Space group	$P2_1/n$	$P2_1/a$	$C2/c$	$P2_1/n$	$P2_1/n$	$P\bar{1}$
Z	4	2	4	2	2	1
a/Å	44.71	9.140	32.532	17.071	12.403	7.537
b/Å	7.85	5.684	5.651	6.011	8.690	8.358
c/Å	6.03	20.672	22.105	22.299	17.871	17.006
α/deg						89.70
β/deg	90.8	97.78	131.5	93.20	100.79	89.68
γ/deg						75.90
τ^a/deg	66	55				
ϕ^b/deg	23.5	41.5	28.7	38		67
$D_c{}^c$/Mg m^{-3}	1.553	1.55	1.325	1.26	1.262	1.291
Volume/Å^3	2116.5	1064.2	3050.8	2284.7	1892.1	1038.9

$^a\tau$, herringbone angle. $^b\phi$, tilt angle of the long molecular axis with a. ^cD_c, calculated density.

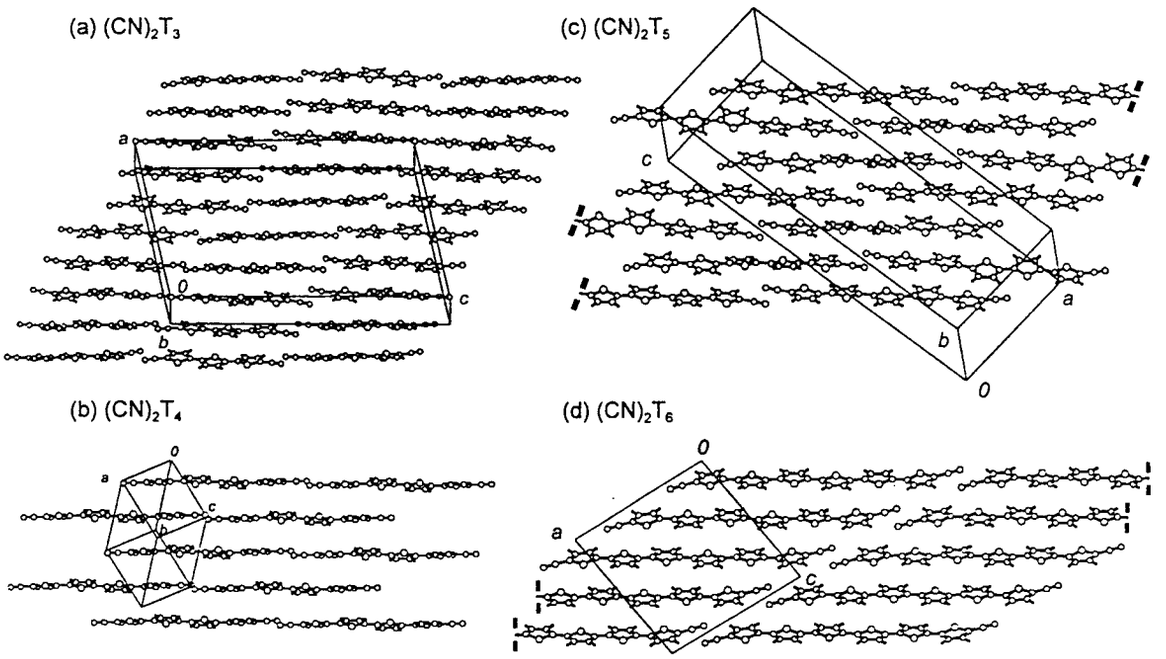

Fig. 4 Comparative packings of α,ω-dicyano substituted oligothiophenes of various lengths: (a) α-3T(CN)$_2$, (b) α-4T(CN)$_2$, (c) α-5T(CN)$_2$ and (d) α-6T(CN)$_2$.[81] (Reprinted with permission from *Chem. Mater.*, 1997, **9**, 981. Copyright 1997 American Chemical Society).

α-3T(CN)$_2$, α-4T(CN)$_2$ and α-5T(CN)$_2$ are stacked in coplanar layers (π-stacks) while α-6T(CN)$_2$ adopts a herringbone motif (Fig. 4).

α-Octithiophene (α-8T). α-8T (Scheme 13) is the longest non-substituted oligothiophene that can be isolated as a pure compound (melting point = 370 °C).[82] But only a few reports deal with α-8T due to the difficulty in purifying it. Nevertheless, α-8T has been characterized as a p-type semiconductor in field-effect transistors[83] and photovoltaic devices.[35–38] Its linear and nonlinear optical properties have also been studied in polycrystalline thin films.[19,84–86]

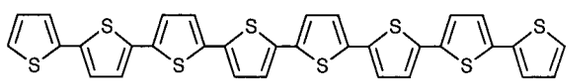

Scheme 13

α-8T crystals of a few millimetres can be obtained by slow vacuum sublimation of the powder material at 300 °C over 24 hours.[60] α-8T crystallizes in the monoclinic system (space group $P2_1/a$) although it is very close to the orthorhombic one (Table 1). The b and c lattice parameters of α-8T are almost similar to those of α-6T while the a-axis is much longer for α-8T (58.916 Å) than for α-6T (44.708 Å). The calculated density of α-8T ($D = 1.578$ g cm^{-3}) is slightly higher than that of α-6T ($D = 1.553$ g cm^{-3}). Such an increase of the packing coefficients with the chain length have been theoretically predicted by Gavezzotti and Filippini.[47] These authors attributed this dependence to the fact that the molecules are roughly brick-shaped and the larger the block the more efficient is the space occupation. A typical view of the α-8T unit cell is represented in Fig. 5. The angle between the planes of two neighbouring molecules is 65° and that between the long molecular axis and the a-axis of the cell is 24°. At the macroscopic scale, the surface of the crystal corresponds to the bc plane.

Table 4 gives the minimum distances between atoms of two face-to-face molecules A and B in the α-8T unit cell and the distances between the nearest ends of two molecules A and B in the same alignment. It can be observed that these distances are shorter by $3–6 \times 10^{-2}$ Å for α-8T and could result in slightly greater intermolecular interactions. Such a crystal packing could in turn improve transport properties in a direction perpendicular to the main molecular axis as compare to α-6T (see section 3.1).

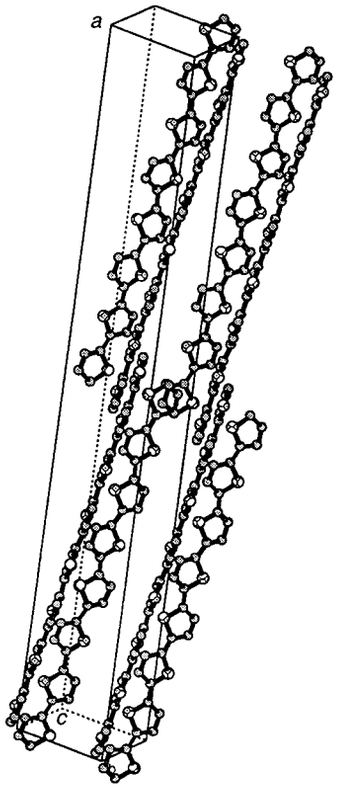

Fig. 5 Crystal packing of α-8T viewed with the *a* axis vertical. Reproduced with permission from ref. 60.

Table 4 Minimum distances between atoms of two neighbouring molecules A and B situated (a) face-to-face and (b) aligned along the same line. From ref. 60

α-8T		α-6T	
(a) Face-to-face			
C_{18}(A)–C_{20}(B)	3.53 Å	C(A)–C(B)	3.56 Å
C_{18}(A)–S_5(B)	3.75 Å	C(A)–S(B)	3.80 Å
S_4(A)–S_4(B)	4.13 Å	S_3(A)–S_3(B)	4.19 Å
(b) Aligned			
C_{32}(A)–C_1(B)	3.80 Å	C_{24}(A)–C_1(B)	3.82 Å

2.1.3 Polythiophene and 3-alkylated derivatives. Although bulk crystals of polythiophenes have never been prepared, a number of structural studies have appeared on their crystallinity in powder form and thin films. Two conformations of the PT chain are possible: a linear and nearly planar all-*trans* structure (rod conformation) and a helical all-*cis* one (coil conformation). Both these geometries, which are separated by an energy barrier of about 3–6 kcal mol^{-1}, have been proposed on the basis of X-ray diffraction studies depending upon substitution and doping state of polythiophene.[62,87] But for a crystal model to be coherent, the polymer chain conformation must be compatible with its packing. Mo *et al.*[62] investigated the X-ray scattering of chemically coupled PT and found that neutral PT can fit either an orthorhombic or a monoclinic unit cell. Further experimental studies including scanning tunneling microscopy provided visual evidence of microcrystalline and helical polymer chain growth.[88,89] Inganäs *et al.* also report on the *syn* conformation in some segments of polythiophene.[90,91] Other experimental studies on the crystal structure of polythiophenes have been reported.[92–94] Mardalen *et al.* report a crystallinity of 10% for stretched oriented alkylated-PTs.[95]

From a theoretical point of view, Cui and Kertesz have studied the geometrical and electronic structures of PT and PMeT by energy band theory where a screw axis of symmetry has been taken into account.[63] These authors confirm that the *anti* (rod) structure is slightly more stable for PT while the *syn* (coil) conformation is preferred for PMeT. Finally, Ferro *et al.* applied molecular mechanics to obtain a monoclinic model of crystalline PT.[64] Their calculations show the weak dependence of packing energy on the unit cell parameter β, *i.e.* on the relative length of adjacent PT chains, in agreement with centrosymmetric and translationally disordered planar chains.

2.2 Polycrystalline thin films

The aim of this section is to describe briefly the preparation and morphology of oligothiophene thin films, keeping in mind their use in planar electronic devices. It is intended to provide a link between the ideal crystal structures described in the previous section and what is experimentally determined in crystalline thin films. Therefore, we will only give the general trends of the most important materials (essentially α-6T and α-8T).

2.2.1 Vacuum deposition. Since non-substituted α-*n*Ts are poorly soluble in organic solvents but are thermally stable, they are essentially handled by vacuum deposition techniques. These techniques allow the control of *both* the thickness of the organic layer and its morphology (orientation, texture, density). Furthermore, the use of ultrahigh vacuum (UHV) brings the additional advantage of an atomically clean environment thus opening the door to high purity materials and devices. Nevertheless, UHV processes like organic molecular beam deposition (OMBD) are expensive and difficult to master. Most of the studies and device fabrications reported in this review have been performed under secondary vacuum (10^{-5} to 10^{-7} torr) in standard vacuum chambers.

The influence of deposition conditions on the α-*n*Ts thin films morphology and properties has recently been summarized.[96,97] In a typical experiment, the α-*n*T powder is introduced in a tungsten boat and heated up to its sublimation temperature under vacuum. Beside the vacuum level and chemical purity of the source material, the main physical parameters to control in order to obtain thin films of the desired quality are the deposition rate and the substrate temperature. Fast deposition rates (a few nanometres per minute) combined with a substrate kept at room temperature usually produce non-oriented films with crystallites of small size (below 100 nm). In contrast, slow rates (a few Å per minute or lower) and a heated substrate tend to produce oriented films with larger grains (up to several microns in diameter).

2.2.2 α-6T and α-8T thin films. Fig. 6 shows scanning electron microscopy (SEM) photographs of α-8T thin films vacuum deposited under various conditions. Fast deposition on a substrate kept at room temperature affords non-oriented films constituted of small crystallites with a size of 50–100 nm (Fig. 6a). In contrast, slow deposition on a substrate heated at 175 °C produces highly oriented films made of larger crystallites with a size around 1 μm (Fig. 6b). Higher magnification (Fig. 6c) reveals an interconnected steps-and-terraces morphology at the origin of increased mobilities (see section 3.1.1). The absorption spectra of the latter films are dichroic ($R=10$ at λ_{max}) indicating that the α-8T molecules are standing upright on the substrate. Fig. 6d shows an α-8T film deposited in three successive steps including a mechanical rubbing step.[37,38] This process allows the alignment of the α-8T molecules horizontally on the substrate with their main axis parallel to the rubbing direction. UV–visible absorbance of the latter films is then considerably increased and absorption spectra are strongly dichroic (Fig. 7). This technique has been applied to photovoltaic diodes in order to increase light absorption by the α-8T layer (see section 3.2).

In the case of vacuum deposited α-6T films, X-ray studies

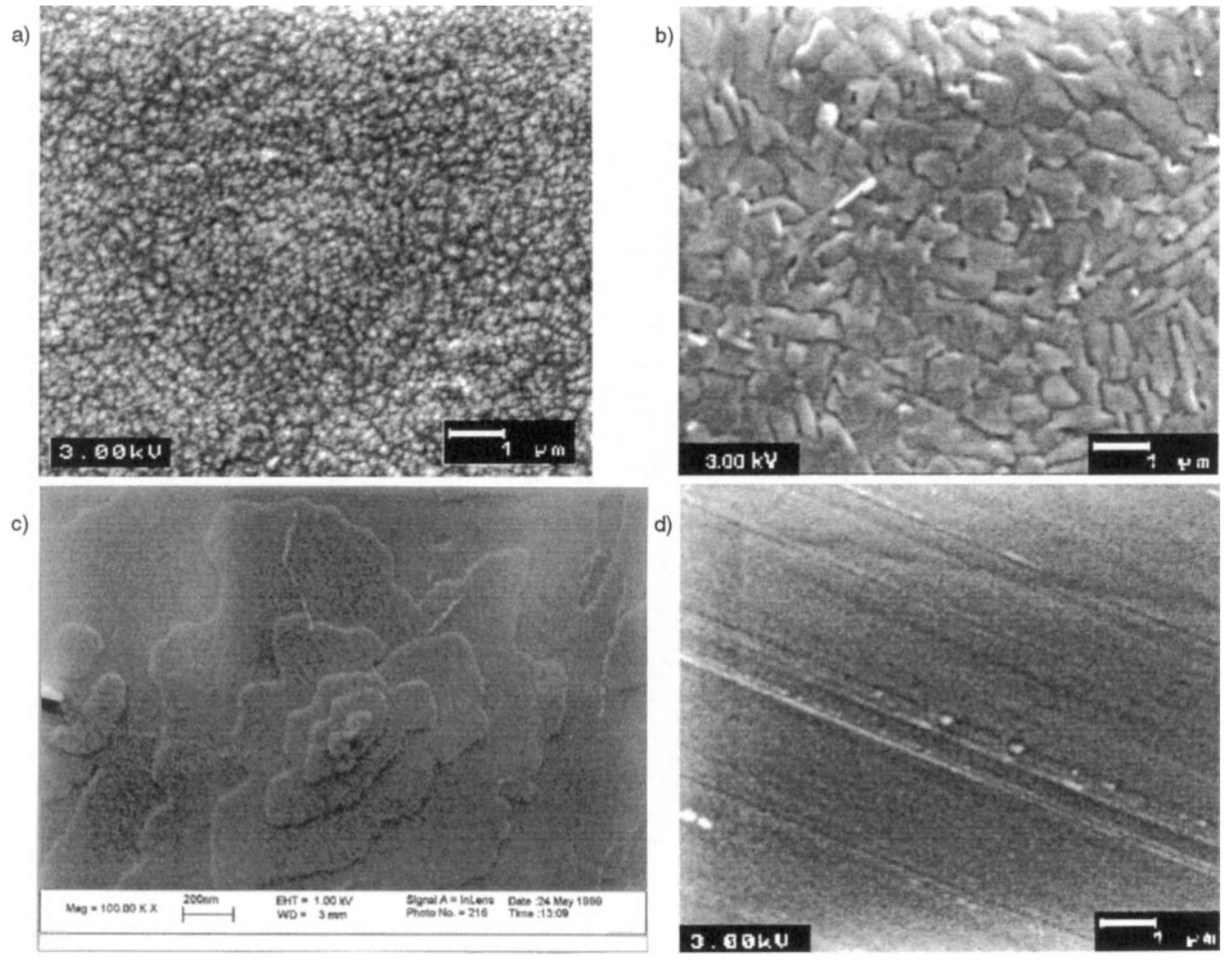

Fig. 6 SEM pictures of α-8T thin films of the same thickness (50 nm) deposited onto a quartz substrate (a) kept at room temperature, (b and c) heated at 175 °C, and (d) using the rubbing technique described in ref. 37, 38. The white scale index in the lower right corner of the pictures corresponds to 1 μm (a, b, d). Magnification of micrograph (c) is 5 times higher than that of (b).

based on meridional 00l reflections show evidence for various crystalline phases depending on the deposition rate and substrate temperature.[51] A substrate kept at room temperature combined to a fast deposition rate (10 nm s^{-1}) leads to two distinct monoclinic phases, a stable α-phase and a metastable β-phase. The β-phase is observed at 77 K and the molecules lie parallel to the substrate. At higher temperatures the crystals grow with their (*a*,*b*) face parallel to the substrate, molecules being thus oriented vertically. Films deposited at 77 K present a uniform surface consisting of very small crystalline grains (10–30 nm). At 300 K, the film morphology consists of isotropic grains more or less separated from each other, with grains size of 50 nm. At 533 K, the grains are larger and rather elongated (30×200 nm^2). The substrate temperature also affects the spacing distance between α-6T molecular layers as well as the tilt angle θ_t between the main molecular axis and the surface normal ($\theta_t = 23°$ at 463 K and $\theta_t = 0°$ at 533 K). Similarly, Biscarini *et al.* report a transition from grains to lamellae over the 300–448 K temperature range.[98]

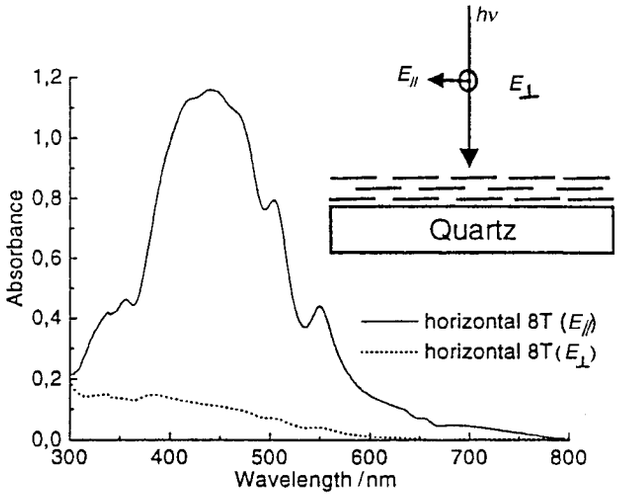

Fig. 7 Absorption spectra of a rubbed α-8T thin film deposited on quartz recorded under normal incidence with light polarized parallel ($E_{\|}$) and perpendicular ($E_{\perp}$) to the rubbing direction. Reprinted from a manuscript submitted to *Solar Energy Mater.*, C. Videlot, A. El Kassmi and D. Fichou, Copyright (1999), with permission from Elsevier Science.

2.2.3 Substituted oligothiophenes. The morphology of α-6T(Hexyl)$_2$ thin films evaporated on a substrate at 300 K has been determined by Lovinger *et al.* and consists of longer and well interconnected crystallites.[99] The authors propose molecular models of the crystalline lattice of α-6T(Hexyl)$_2$ and their sub- and supramolecular correspondence to the dark and light electron microscopic morphological features (Fig. 8).

The morphology and transport properties of dialkylated anthradithiophenes also show a marked dependence on the substrate temperature as shown by Laquindanum *et al.*[100]

2.2.4 Influence of substrate nature. Beside the physical conditions of deposition, the chemical nature of the substrate plays an important role on the molecular orientation of oligothiophenes thin films. Ordered monolayers of various

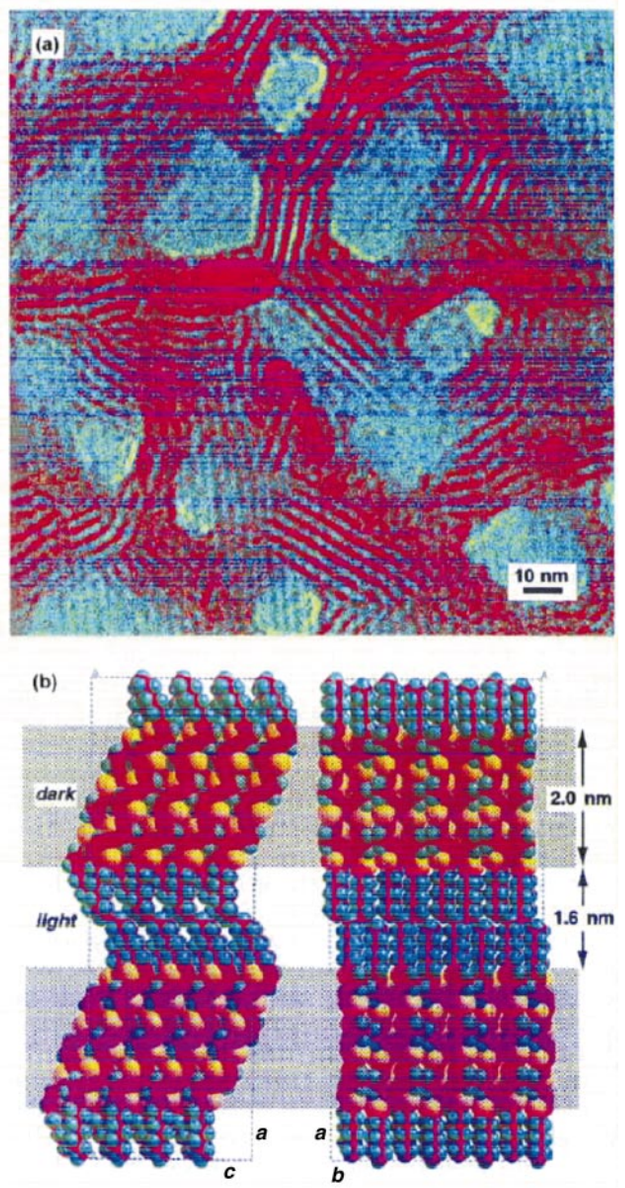

Fig. 8 (a) Morphology of a α-6T(Hexyl)$_2$ thin film as observed by bright-field transmission electron microscopy and (b) molecular models of the crystalline lattice of α-6T (Hexyl)$_2$ and their sub- and supramolecular correspondences to the dark and light electron microscopic morphological features.[99] (Reprinted with permission from *Chem. Mater.*, 1998, **10**, 3275. Copyright 1998 American Chemical Society).

oligomers have been deposited on noble metals (Ag, Au). From a general point of view, oligothiophenes lie horizontally on noble metal surfaces because of preferential bonding to the metal *via* the π-backbone. The use of noble metals seems to be an essential stage toward highly ordered films of lying oligomers. In fact, on these surfaces no molecular dissociation occurs and bonded molecules still have lateral mobility for two-dimensional (2D) ordering. Ultrathin films of α-4T were deposited onto Ag(111) by vacuum sublimation and characterized.[101] For the mono-layer, a long range order superstructure was observed by electron diffraction. This is commensurate (relaxed) with the Ag(111) surface due to covalent bonding of the molecules *via* its π-system. For multilayers (between 3 and 20 layers) a gradual decrease of the orientational order is observed. More recently, an exhaustive study of superstucture formation on Ag(111) is reported by Soukopp *et al.*[102] A series of "end-capped" α-*n*T with different chain lengths ($n=3$–6) were vapor deposited onto Ag(111) surface. The adsorption and structural ordering were investigated by thermal desorption spectroscopy, and low energy diffraction as well as scanning tunneling microscopy. The authors observed highly ordered mono-layers with molecules lying horizontally and long range ordered domains of several hundred Å diameter, for all molecules. 2D-ordering of α-6T was also observed on single crystal Au(111).[103] As in the case of Ag(111) α-6T orients parallel to the Au rows. In the first monolayer the molecules form a $(T\times 4)$ super-structure. Again, a gradual decrease of the orientational order is observed for multi-layer structures.

For inert surfaces like graphite or MoS_2 one expects a high degree of self organization because of their weak (physisorption) coupling to the substrate.[104] Orientation parallel to the substrate is also observed when α-*n*T are vacuum deposited onto stretched polyethylene.[105] The molecules lie with their long axes parallel to the stretching direction, thus forming a highly anisotropic medium. Borghesi *et al.* have grown thin films of alkyl-substituted α-6T (615 Å) by OMBD on (001)-oriented potassium acid phthalate crystals.[106] The precise control between van der Waals intermolecular forces and the first monolayer–substrate interaction allows the preparation of highly ordered films.

2.2.5 Solution deposition. A few substituted α-*n*Ts are soluble and can be processed from solution by spin coating, casting, self-assembly, Langmuir–Blodgett or electrochemical techniques. These methods essentially apply to oligomers substituted by alkyl or alkoxy chains or to short substituted oligomers. Unfortunately, most of these materials are not suited to device applications and will not be addressed in this section. Beside the preparation of bulk films, guest–host thin films have also been prepared by incorporating the oligomer into a well-defined matrix such as nematic liquid crystals,[107] zeolites.[108,109]

3 Effect of crystal order on opto-electronic devices

3.1 Field-effect transistors

Over the last five years, there has been a considerable interest in field-effect transistors (FETs) based on small conjugated molecules. Mobilities in the range $\mu=0.01$–$1.0\ cm^2\ V^{-1}\ s^{-1}$, *i.e.* close to that of amorphous silicon, and I_{on}/I_{off} ratio of the order 10^6 to 10^8 have been obtained in FETs based on pentacene,[110,111] sexithiophene[12,27,112,113] and octithiophene.[83,114] Organic FETs now obviously meet some of the requirements for applications for which low switching speeds are required, like for example active matrix displays and smart cards. One essential finding is that both the I_{on}/I_{off} ratio and the mobility can be improved by a proper molecular design and precise control of crystalline ordering.[26,78]

3.1.1 Thin film transistors (TFTs). Field-effect transistors based on various oligothiophenes thin films have been reported in the literature these last ten years, for example in the case of

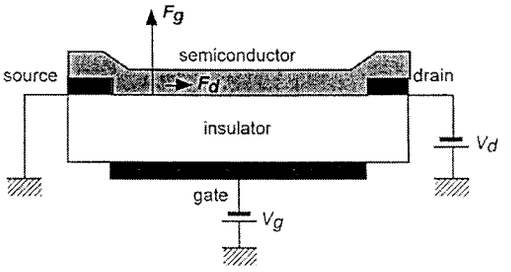

Fig. 9 Typical schematic structure of an organic FET.[114] (Reprinted with permission from *J. Appl. Phys.*, 1999, **85**, 3202. Copyright 1999, American Institute of Physics).

α-3T,[115,116] α-4T,[116–119] α-5T,[115–118] α-6T[11,51,78] and α-8T.[83,115] Transistors have also been fabricated with random-regular[120] and regio-regular[121,122] poly[3-alkylthiophenes]. A typical organic FET architecture is shown in Fig. 9. Carrier density is estimated from classical equations of the field-effect mobility and conductivity. For example, the carrier density in α-6T was estimated to be in the range $\mu = 10^{14}$–10^{15} cm^{-3}.[21,23] High purity α-6T films and single crystals possess much lower carrier concentrations (typically 10^{11} cm^{-3}).[75] The FET mobility of oligothiophenes increases along with three parameters: 1) oligomer length, 2) chemical purity of the layer and 3) crystalline order. In particular, the degree of ordering in the film has a crucial importance on the FET's performance.

In α-6T TFTs, charges are assumed to travel essentially along the stacking axis which therefore must be oriented parallel to the substrate plane to ensure high channel mobility. As stated in section 2.2, films prepared by deposition at room temperature consist of small crystallites (50 nm) and consequently low mobility (2×10^{-3} cm^2 V^{-1} s^{-1}) have measured in these films.[51] The mobility is even reduced to 6×10^{-3} cm^2 V^{-1} s^{-1} when the substrate temperature is decreased to 77 K during deposition, due to impurity adsorption on the film and a smaller crystallite size (10–30 nm). Above 533 K, larger crystallites (30×200 nm^2) are formed leading to mobility as high as 2.5×10^{-2} cm^2 V^{-1} s^{-1}.

We have seen in section 2.1.2 that the crystal packing of α-8T could improve the charge transport perpendicular to the main molecular axis as compared to α-6T due to a slightly higher density. This assumption has been verified recently with α-8T based thin film transistors (TFTs). Hole mobilities in the range 0.06–0.09 cm^2 V^{-1} s^{-1}, *i.e.* three times higher than in α-6T-TFTs, have been measured with high purity and oriented α-8T-TFTs.[83] A record mobility of 0.2 cm^2 V^{-1} s^{-1} has been obtained during the preparation of this review by heating the TFT substrate at 175 °C during α-8T deposition (see section 2.2.2).[123] This higher substrate temperature produces much bigger α-8T crystallites with a size of approximately 1 μm (instead of 50–100 nm at 150 °C) as it is illustrated in Fig. 6b. However, these high mobilities may also find their origin at the molecular level, α-8T having a longer π-conjugated chain than α-6T. A comparative study of TFTs based on α-4T, α-6T and α-8T clearly shows that 8T definitively possesses the highest mobility of the three oligomers investigated.[114] This is illustrated in Fig. 10 where the field-effect mobility is given as a function of the gate voltage.

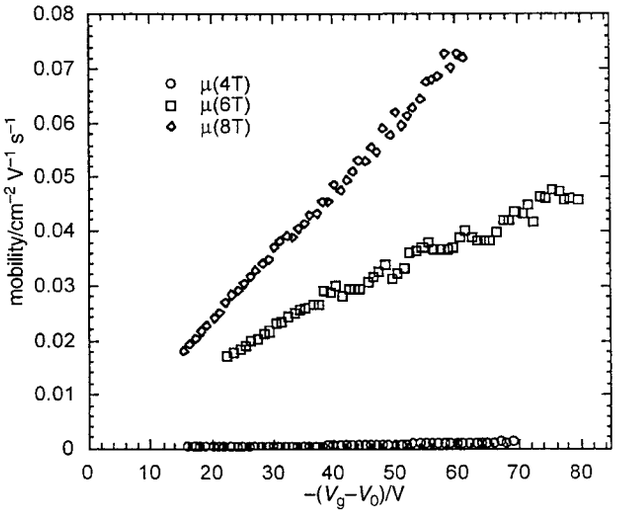

Fig. 10 Variation of the mobility corrected for the series resistance as a function of the gate voltage for α-4T, α-6T, and α-8T.[114] (Reprinted with permission from *J. Appl. Phys.*, 1999, **85**, 3202. Copyright 1999, American Institute of Physics).

3.1.2 Single crystal transistors. Macroscopic single crystals (of millimetre dimensions) offer the possibility to elucidate the intrinsic transport properties as well as electrical anisotropy, thus avoiding grain boundary and interface effects. Because most oligothiophenes crystals grow as ultra-thin and brittle lamellae of small size (*i.e.* usually less than a millimetre), their handling is extremely delicate and their physical studies very restricted. Nevertheless, a few optical and electrical properties of non-substituted α-6T and α-8T crystals grown by sublimation have been investigated over the last two years.

Field-effect transistors (FET) built with α-6T crystals playing the role of the semiconductor have been fabricated.[112] In these devices, an α-6T single crystal (5 microns thick) is carefully deposited on top of a PMMA layer (the insulator) which is itself spin-coated on an aluminum gate electrode. The device is completed by two gold source and drain electrodes. A field-effect hole mobility of 0.075 cm^2 V^{-1} s^{-1} is then recorded at room temperature, *i.e.* roughly three times greater than that of α-6T polycrystalline thin films. The on–off ratio above 10^4 is mainly limited by leaks through the insulator. The current–voltage characteristics of this FET allows the estimation of the dopant concentration in the α-6T crystal as 0.2 ppm and a free carrier density of 10^{11} cm^{-3}. These results are consistent with the high degree of purity of the material. An even higher field-effect mobility (0.16 cm^2 V^{-1} s^{-1}) has been reported recently for the α-6T crystal.[27] According to the authors, this could be due to the use of a very small crystal as well as its low doping level. Nevertheless, it is not possible in this device geometry to measure the anisotropy of the mobility in the α-6T crystal but it can be anticipated that it is much higher in the direction perpendicular to the long axis of the molecule, *i.e.* between the source and drain electrodes of the transistor.

As described in section 2.1.2, α-6T crystallizes in two different phases depending on the growth temperature (HT and LT). The α-6T/HT phase allows a larger overlap of the π-orbitals resulting in a higher mobility $\mu = 0.5$ cm^2 V^{-1} s^{-1}, *i.e.* more than twice the value obtained for the low temperature α-6T/LT phase.[75] Schön *et al.* evaluated the mobility anisotropy in single crystals of α-4T and α-6T.[75,124] The strong anisotropy is a direct consequence of both the molecular and structural anisotropies themselves. In the crystal, the molecules are aligned in a parallel fashion and form superimposed molecular planes into which charges are travelling. This arrangement involves a more important overlap of π-orbitals in the molecular plane compared to the direction perpendicular to

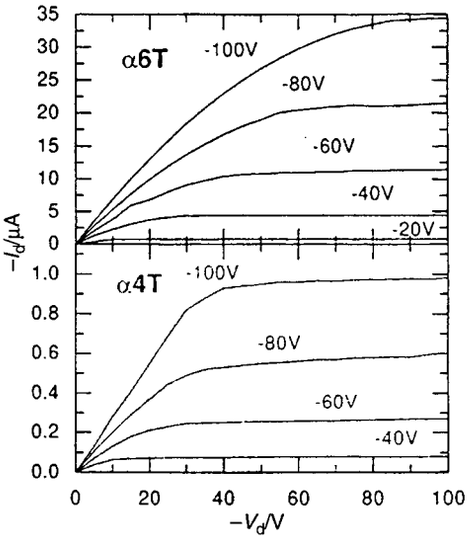

Fig. 11 Drain current *vs.* source-drain voltage for different source gate voltages of an α-6T (top) and an α-4T single crystal FET (bottom).[124] (Reprinted with permission from *Appl. Phys. Lett.*, 1998, **73**, 3574. Copyright 1998, American Institute of Physics).

this plane. Schön *et al.* also measured the conductivity parallel ($\sigma_{\parallel}$) and perpendicular ($\sigma_{\perp}$), corresponding respectively to high and low mobility directions in the crystals. Fig. 11 shows typical I_D–V_D characteristics of α-4T and α-6T single crystals transistors. Conductivity values of 5×10^{-11} and 6×10^{-13} S cm^{-1} are recorded. The anisotropy ratio ($\sigma_{\parallel}/\sigma_{\perp}$) was found to be 80 for α-6T crystals and 70 for α-4T crystals. These values are higher than those reported for well oriented α-6T thin films.[51] Schön *et al.* also report on the bulk mobility of the crystals as determined from space charge limited current in the free trap regime. Values up to $\mu=0.46$ and $\mu=0.06$ cm^2 V^{-1} s^{-1} have been estimated for conduction parallel to the growth surface in α-6T and α-4T respectively.

An alternative method to measure the field-effect mobility of oligothiophenes single crystals is to grow them directly on top of a transistor device by slow vacuum evaporation. One of the advantages of this method is that the metallic contacts as well as the interface between the semiconducting crystal and the insulator are of better quality as compared to what they currently are in devices using a macroscopic crystal deposited on top of the insulator. Another advantage of controlling the growth of the crystal directly on the FET device is that it allows checking of the transport properties along the various crystal axes. This technique has been recently used by Schoonveld *et al.* to study the intrinsic charge transport properties of α-4T thin films with crystallites having diameters up to 20 μm[125,126] and is currently under way for α-6T.[127] Fig. 12 shows the multi-terminal α-4T single crystal transistor where the crystal is located at the center of the eight contacts. The experiment excludes the effects of grain boundaries and contact resistance and leads to a carrier mobility of 1.2×10^{-3} cm^2 V^{-1} s^{-1} for the α-4T single crystal. Note that Vrijmoeth *et al.* also developed a method to determine the crystal axis direction and thickness of the individual α-4T crystals by polarization spectroscopy.[128]

3.1.3 Other thiophene-based transistors. *α,ω-Bis-silylated thiophene oligomers.* The FET characteristics of a new family of α,θ-bis-silylated thiophene oligomers having a normal crystal structure have been described by Barbarella *et al.*[129] These compounds crystallize in a triclinic cell (with $Z=1$ or $Z=2$ depending on the molecular structure) and adopt a sandwich-type molecular packing referred as π–π stack. The molecular π–π stack of these compounds does not contain any van der Waals contact less than 3.6 Å. The shortest S···S intermolecular distances, *i.e.* a determinant parameter for transport properties in molecular crystals, are in the range 4.2–4.6 Å. The best FET performance is achieved with the α,ω-bis-silylated pentamer, which has a mobility of 3×10^{-4} cm^2 V^{-1} s^{-1}. This illustrates clearly the importance of crystal arrangement, particularly the interplay between intermolecular distances and the packing geometry (herring-bone or π–π stack) on the FET performances. Efficient FET materials can then be designed by combining short intermolecular distances together with a π–π stack-like arrangement.

Bi(dithienothiophene). Sirringhaus *et al.* report on high FETs performances using bi(dithienothiophene) (BDT), a material corresponding to the above mentioned approach.[130] The BDT-FETs show exceptionally high on/off ratios up to 10^8 between accumulation and depletion regimes, mobilities in the range $\mu=0.02$–0.05 cm^2 V^{-1} s^{-1} and sharp turn-on characteristics comparable to that of a-SiH-FETs. These good performances are attributed to the favourable coplanar π–π stack. BDT has a monoclinic unit cell with space group $C2/c$. The cell parameters are $a=33.689$ Å, $b=3.883$ Å, $c=11.106$ Å and $\beta=101.093°$. The molecular planes are strictly parallel thus resulting in a stronger π–π overlap between adjacent molecules.

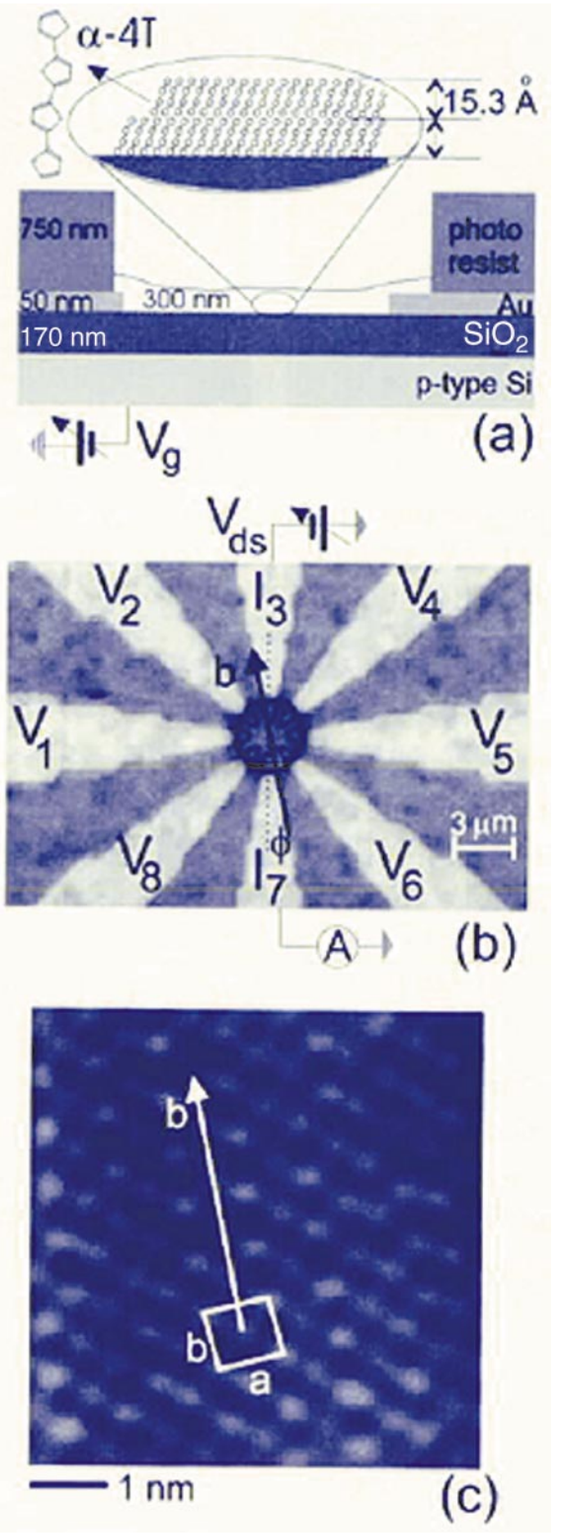

Fig. 12 Multi-terminal transistor based on a α-4T single crystal up to 40 μm in diameter. (a) schematic structure, (b) top view and (c) AFM image of the crystal sample.[126] (Reprinted with permission from *Appl. Phys. Lett.*, 1998, **73**, 3884. Copyright 1998, American Institute of Physics).

Regioregular poly(3-hexylthiophene). The first reported FETs based on polythiophene has been reported by Tsumura *et al.*[13] and Assadi *et al.*[14] The extremely low mobilities ($\mu=10^{-5}$ cm^2 V^{-1} s^{-1}) found in these FETs can be ascribed to the high structural disorder of the PT materials. Since then, McCullough *et al.* have described a reproducible method to afford highly ordered regioregular poly(3-alkyl-thiophenes).[131,132] The transport properties of regioregular

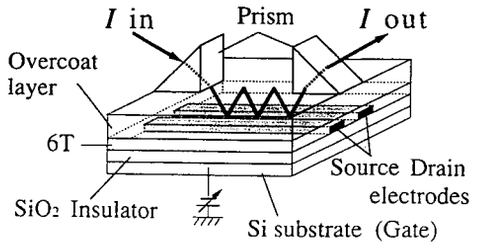

Fig. 13 Structure of a field-effect transistor-type waveguide device using α-6T as the semiconductor. Reprinted from *Thin Solid Films*, 1998, **331**, 55, T. Kurata *et al.*, Copyright (1998), with permission from Elsevier Science.

poly(3-hexylthiophene) (PH3T) have been studied by Bao *et al.* in FETs.[121,133] Mobilities as high as $\mu = 0.05\ cm^2\ V^{-1}\ s^{-1}$ and on/off ratios close to 10^4 are reported. An all-polymer FET-LED tandem device based on PH3T has also recently been reported by Sirringhaus *et al.*[122] This dual device exhibits high mobility (0.05–0.1 $cm^2\ V^{-1}\ s^{-1}$, with on/off ratio of 10^6) while driving a MEH-PPV-based light emitting diode. The high mobility in regioregular PH3T is attributed to the formation of extended polaron states as a result of self-organization in the films. X-Ray diffraction shows a diffraction peak at 5.4° corresponding to an intermolecular spacing of 16.36 Å between the chains of the well organized lamellar structure. However, electron diffraction shows a single peak at 3.7–3.81 Å attributed to the distance between thiophene rings of neighboring chains. These short distances are very close to those found in single crystals of α-6T or α-8T thus explaining the efficient transport properties of regioregular P3HT.[133]

Finally, field-effect transistors can be used in an hybrid structure to design electro-optical waveguides.[134] However the modulation ratio remains low (about 5%) and the origin of modulation is not clear. Recently, Kurata *et al.* have fabricated an efficient optical waveguide modulator with a FET-type electrode using α-6T as the semiconductor.[135] This device operates as an electro-absorption modulator with a modulation ratio as high as 20% (see Fig. 13). This high modulation ratio is a direct consequence of the weak absorption and scattering of the α-6T films in its transparency region. The α-6T film must then be deposited according to the conditions described in section 2.2, *i.e.* using a fast deposition rate (100 Å min^{-1}) and a substrate kept at room temperature.

3.2 Photoconductivity and photovoltaic cells

Organic photoconductors are now widely used materials in xerography and laser printing.[136] These natural or synthetic dye stuffs can be easily coated as flexible layers and possess spectral sensitivities spanning the entire visible (and near infrared) range. Photoconductivity in organic semiconductors can also be used to design photovoltaic diodes (or solar cells). This second type of application, which is based on metal-semiconductor (MS) junctions or p/n heterojunctions made of organic thin films as the active materials, has not yet reached the industrial stage due to too low power conversion efficiencies (up to 1–2%). Nevertheless, rapid progress in organic solar cells has been made over the last few years and applications to large panels as well as high-tech niche applications can already been envisaged.

The main organic dyes used in xerography (phthalocyanines, hydrazone derivatives, azo and squarilium pigments, *etc.*) or under investigation for solar cells (phthalocyanines, porphyrines, *etc.*) are well-known and commercial materials. Since the oligothiophene family is more recent, their photoconductive and photovoltaic behaviours have not yet been completely elucidated. We summarize in this section the recent advances that have been reported on this topic, concentrating essentially on α-6T and α-8T.

Photoconductivity of oligothiophenes. The photoconductivity (PC) in α-6T polycrystalline thin films has been measured by Dippel *et al.* showing that its quantum yield increases from 2.1 to 2.6 eV while the PL yield drops by a factor of 20 over the same excitation energy range.[137] The PC spectrum is antibatic with the PL excitation spectrum. This unusual behaviour of molecular solids is interpreted in terms of energy-dependent branching between PL and dissociation of a singlet excitation into weakly bound electron-hole pairs. Zamboni *et al.* report on the PC action spectrum which exhibits a broad band peaking at 520 nm in the visible range.[138] The comparison between photoexcitation and PC action spectra suggests that they are qualitatively complementary. The two spectra cross each other at approximately 544 nm, *i.e.* at approximately the same energy where the 2^1A_g exciton band is observed. In the case of α-6T single crystals grown from the vapor phase, the PC action spectrum first correlates the absorption onset at 2.4 eV and then exhibits a second rise at 3.0 eV up to a maximum at 3.3 eV.[139] The first rise is attributed to the generation of singlet excitons which then give birth to charges through either exciton breaking or more likely charge detrapping. As observed in polycrystalline thin films, PL and PC action spectra of crystals show inverse behaviors, the former exhibits a minimum at 3.5 eV, whereas a maximum is found at this energy in the latter. The second rise at 3.3 eV could be explained by "direct ionisation", *i.e.* a second more efficient mechanism of charge generation. In that case the energy difference between the two onsets (0.8 eV) would measure the singlet exciton binding energy. Finally, the authors estimate the PC quantum yield to be around 10^{-3} at the first saturation level.

Comparative transient PC studies have been carried out recently by Moses *et al.* on α-8T single crystals and polycrystalline thin films.[140] The essential purpose of these comparative experiments is to study the intrinsic properties of photoexcitation and transport in model molecular crystal systems and to determine the role of structural defects. Picosecond transient PC measurements over a wide range of temperatures (10–300 K) demonstrate that the dependence of photocurrent on light intensity and electric field in the single crystal α-8T is radically different from that in vacuum-deposited polycrystalline films (Fig. 14). The photocurrent lifetime in the α-8T crystal is of the order of a nanosecond whereas in the film it is less than 100 ps. These observations indicate a bimolecular carrier recombination component prevailing in the α-8T single crystals, whereas a monomolecular mechanism operates in the polycrystalline films.

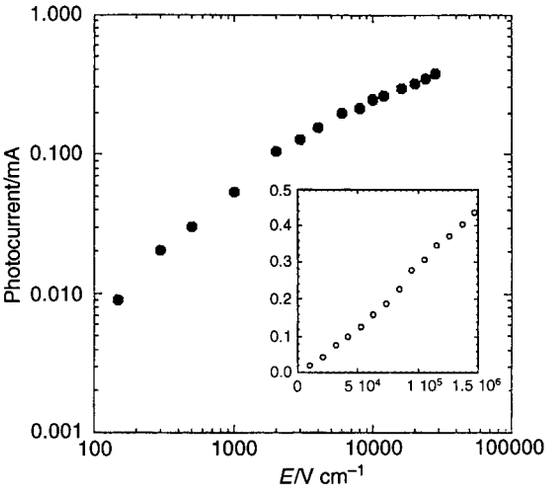

Fig. 14 Field-dependence of the peak transient photocurrent in a α-8T polycrystalline thin film (black dots) and single crystal (inset, white circles). Reproduced with permission from ref. 140, copyright 1999, American Physical Society.

Photovoltaic diodes (solar cells). A number of organic semiconductors including small molecules,[141–146] conjugated polymers,[147–150] liquid crystals[151] and internal donor–acceptor polymer networks[152,153] have been used to design PV cells. In addition, organic PV devices with various architectures have been explored, such as Schottky junctions, two-layer p/n heterojunctions and p–i–n junctions. Hybrid organic–inorganic junctions have also been investigated using conventional semiconductors like GaAs or CdS in contact with a conjugated polymer like polythiophene.[154–156] However, the development of organic solar cells requires a better understanding of light absorption and charge transport mechanisms in organic semiconductors.

In sharp contrast to inorganic semiconductors in which photogenerated electrons and holes are free carriers, organic semiconductors generate bound excitons (electron–hole pairs) which are not willing to dissociate easily. Two approaches have been followed to enhance charge separation in organic PV cells. The first is to use two-layer p–n junction devices while the second is to use a single layer of a donor–acceptor blend called a *bulk D–A heterojunction*. In these D–A blends, the donor moiety has a small ionization potential and good hole transport properties while the acceptor has a high electron affinity and efficient electron transport properties. Following the first approach, Noma *et al.* report the PV properties of the p–n heterojunction cell {ITO/perylene/α-8T/Au}.[35] This cell exhibits fairly good characteristics with a fill factor FF = 0.5 and a conversion efficiency of 0.6% for irradiation of white light at 105 mW cm^{-2}. In the same work the authors report much lower fill factor 0.29 and conversion efficiency 0.02% for a similar cell using α-5T.

The natural upright molecular orientation adopted by the α-8T ribbon-like molecules when deposited on top of glass substrates is not suitable for efficient light absorption. It is thus necessary to align the α-8T dipoles flat and horizontal on the substrate in order to improve light absorption and therefore light conversion efficiency. The most efficient way to achieve horizontal orientation of oligothiophenes on substrates is to adapt the mechanical rubbing technique used to align liquid crystals. Videlot *et al.* have studied the influence of molecular orientation on the photovoltaic properties of α-8T films.[37,38] As expected, photocurrent intensity is tenfold higher for horizontal α-8T, as shown in Fig. 15 for a p/n heterojunction using a perylene derivative as the n-type semiconductor. This improvement is attributed to a more efficient light absorption rather than to better transport properties of the α-8T layer. Nevertheless, the strong absorption dichroism of horizontal α-8T films ($R = 10$) is not retained in action spectra.

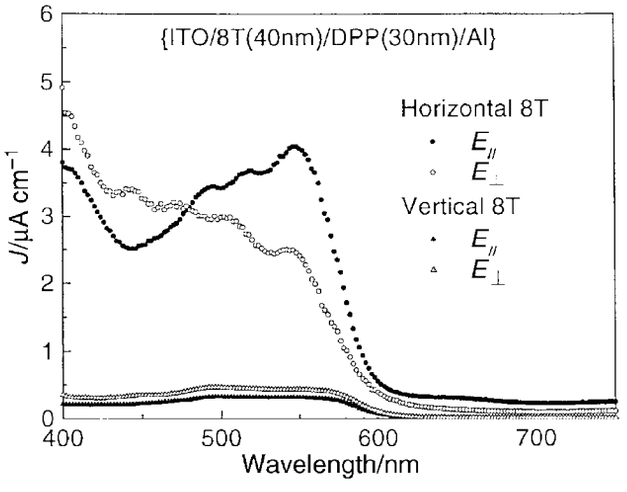

Fig. 15 Photocurrent spectroscopy of two {ITO/α-8T(40nm)/DPP(30nm)/Al} p/n heterojunctions illuminated by polarized light through ITO in short circuit conditions with (a) vertical and (b) horizontal α-8T thin film orientations. Reprinted from a manuscript submitted to *Solar Energy Mater.*, C. Videlot, A. El Kassmi and D. Fichou, Copyright (1999), with permission from Elsevier Science.

The influence of the α-6T film morphology on their photovoltaic properties have been investigated by Marks *et al.*[157] The average size of the crystallites increases with the substrate temperature (from 0.2 μm at 22 °C to 1.5 μm at 150 °C), accompanied by an increase of the structural order within the film. Photocurrent would then result from field-induced exciton dissociation in the bulk rather than charge electrode contacts. Efficiency variations with structural order suggests that traps and defects assist exciton dissociation. Highly ordered films would then be less efficient photodiodes because they contain fewer traps, making charge separation more difficult.

A more efficient exciton dissociation can be realized by distributing the local sites where charge separation takes place in a bulk material. This approach has been developed by a number of groups using different techniques and materials such as poly(3-alkylthiophene) and C_{60}.[158–161] Another promising approach is the two-layer polymer diode fabricated by a lamination technique using substituted polythiophene proposed by Granström *et al.*[162] The structures provide good connection to the electrodes and achieve power conversion efficiency of 1.9% under simulated solar spectrum.

3.3 Light-emitting diodes (LEDs) and laser crystals

The design of organic LEDs requires materials combining high luminescence efficiencies and good transport properties. In the solid state, oligothiophenes generally have low luminescence efficiencies whose origin is probably related to strong intermolecular interactions. Reported values of photoluminescence (PL) efficiency for α-6T polycrystalline thin films are in the range 10^{-4} to 10^{-2}%[163,164] although efficiencies up to 9% have been recently measured on α-4T, α-6T and α-8T single crystals.[140] In the solid state, the intense $1A_g \rightarrow 1B_u$ allowed transition of α-6T splits into two levels (Davydov splitting estimated in the range 10 000–15 000 cm^{-1}), the fundamental transition having an energy of 2.43 eV.[165] Introduction of alkylated substituents on the α-6T backbone modifies intermolecular distances and strongly affects optical spectra and transport properties.[166–170]

Besides, EL requires the injection of both positive and negative charges into the organic layer. Oligothiophenes are efficient p-type semiconductors but the barrier for electron injection from the cathode into the LUMO is higher than the barrier for hole injection from the anode into the HOMO. Consequently, α-*n*Ts polycrystalline thin films can hardly be envisaged as emitting materials in LEDs but rather used as efficient hole transport layers. However, the higher luminescence efficiency of single crystals generates stimulated emission due to a proper dipole alignment.

3.3.1 Light-emitting diodes. From a general point of view amorphous materials based on short oligomers are more efficient for LEDs compared to crystalline longer oligomers or even polythiophenes.[29,30,171–173] For example, a substantial increase of the EL efficiency has been reported by Noda *et al.* for an end-substituted terthiophene derivative (α-3T-BMA) which forms a stable amorphous glass ($T_g = 93$ °C).[174] A similar tendency has also been observed with amorphous glasses based on dimesitylboryl α-2T and α-3T derivatives (α-2T-DMB and α-3T-DMB) which behave as excellent electron transport materials.[175] Up to now, LEDs using α-3T-DMB show the highest EL efficiency (1.1%) reported for an oligothiophene LED.

Along this line, the low degree of crystallinity of polythiophenes (see section 2.1.3) should result in higher luminescence efficiencies compared to highly crystalline

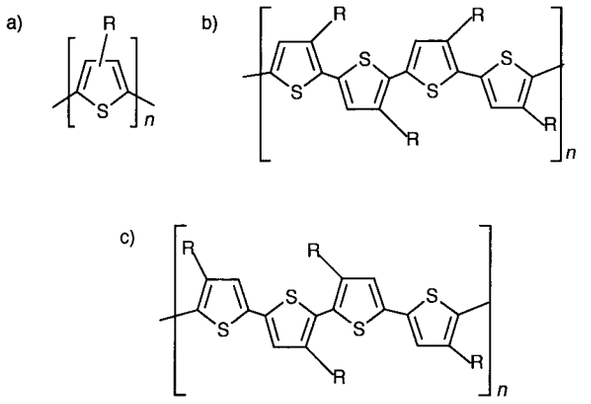

Scheme 14

oligomers.[176–178] Comparative EL studies of regioregular and non-regioregular P3HT (Scheme 14) show that both polymers have low quantum efficiencies in the range 10^{-4} to 10^{-5}%.[179] This indicates clearly that structural order is not a prerequisite for efficient EL. Nevertheless, the precise control of regioregularity in polythiophenes is a powerful tool to tune the EL wavelength.[180] Surprisingly, a higher quantum efficiency is found for head-to-head/tail-to-tail polymers (0.3%).[181]

As for transport properties, crystalline order of the organic layer controls the luminescence properties of LEDs and particularly to produce polarized light, light being emitted in a cone normal to the direction of the emitting dipole. Weakly polarized EL has been observed by Marks *et al.* with α-6T by varying the deposition conditions.[182,183] As shown in Fig. 16, emission is polarized when the substrate temperature is high enough to produce large grains with upright molecular orientation. For polythiophenes, chain alignment can be achieved by stretching to create an anisotropic material. Dyreklev *et al.* report polarized EL from oriented poly(3-(4-octylphenyl)-2,2′-bithiophene) (PTOPT) on stretched polyethylene (PE).[184] As expected, EL is polarized in the direction parallel to the polymer chains. Finally, Bolognesi *et al.* observed polarized EL using oriented poly(3-decyl-4-methoxythiophene) (PDMT)[185] with chain orientation achieved by the Langmuir–Blodgett technique. In spite of a reasonable chain alignment (dichroic ratio = 1.8), the rectification ratio of the multilayered {ITO/PDMT/Al} device is weak and the EL light only slightly polarized ($EL_{\parallel}/EL_{\perp} = 1.3$).

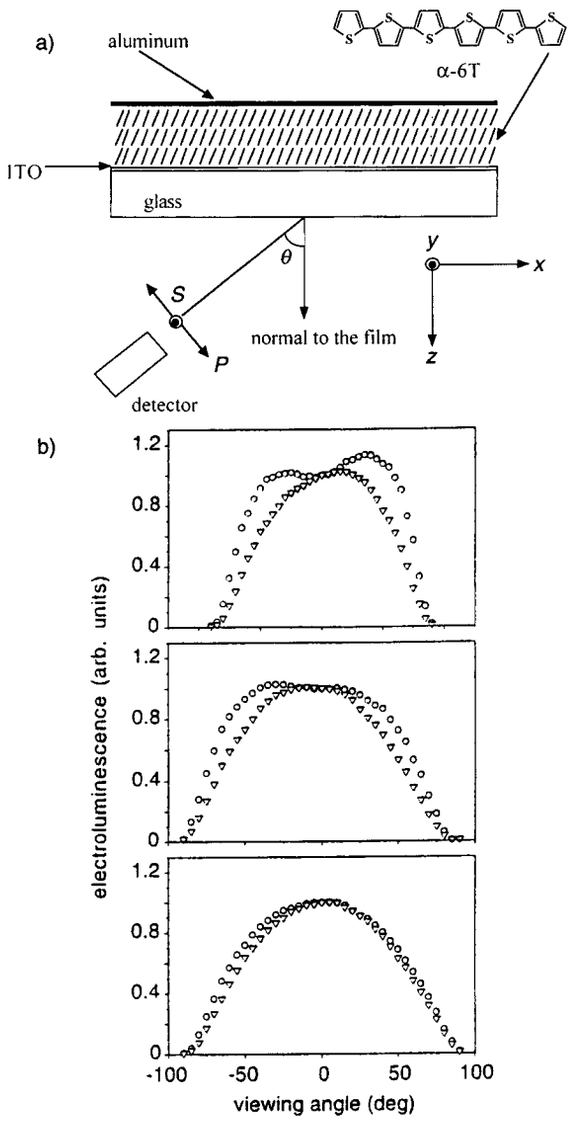

Fig. 16 (a) Measurement of angularly resolved polarized electroluminescence with an upright oriented α-6T LED and (b) angular dependence of EL for devices made at 155 °C (top), 104 °C (centre and 55 °C (bottom) substrate temperature. Open circles correspond to p-polarized and triangles to s-polarized light. From ref. 182.

3.3.2 Laser crystals. An organic laser diode, *i.e.* the ultimate step of the organic LED, has been recently envisaged. In particular, it has been shown that conjugated polymers like PPV and its derivatives could yield stimulated emission (SE) under intense optical excitation. More recently, integration of these polymers in planar optical cavities led to the observation of laser emission under optical pumping. Although it has not yet been possible to produce laser light under electrical pumping, a number of materials and device structures have been investigated. Beside polymer microcavities, it has also been demonstrated that α-*n*T single crystals operate as natural optical cavities. Essential results of these two approaches are summarized below.

The only example of microcavity based on a polythiophene derivative has been recently designed by Granlund *et al.*[186] The emissive organic layer is sandwiched by melt pressing into two distributed Bragg reflectors. Under optical pumping at 530 nm, a lasing threshold is observed at 120 nJ cm^{-2}. Evidence for lasing is mainly found in 1) the sharp increase of emitted intensity at pump energy of 170 nJ cm^{-2}, 2) spectral narrowing down to 1.8 nm and 3) polarization of the emitted light. The gain coefficient is estimated to be $g = 80 \pm 20$ cm^{-1}.

Stimulated emission (SE) has first been observed in single crystals of α-8T under intense photoexcitation at normal

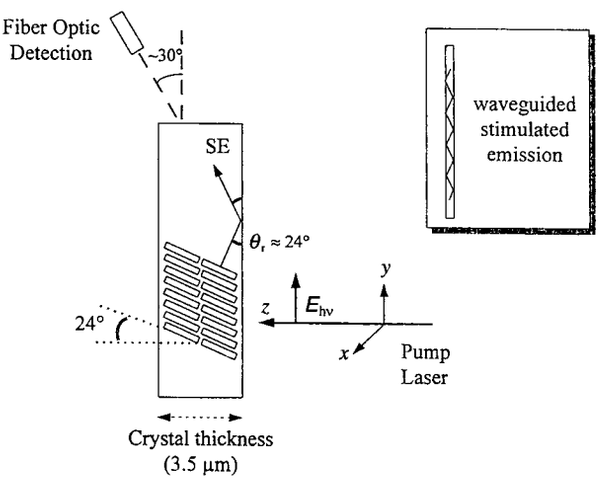

Fig. 17 Experimental arrangement for the observation of waveguided stimulated emission in an ultra-thin α-8T single crystal. Reproduced with permission from ref. 187.

incidence (Fig. 17).[187] Similar SE phenomena have also been observed in α-4T and α-6T crystals.[187–191] SE occurs at a pump energy threshold of ~0.1 mJ per pulse (33 ps, 10 Hz) to yield an intense and narrow emission line peaking at 700 nm for α-8T. At pump energies higher than 15 μJ per pulse, a second narrow line of weaker intensity emerges at 640 nm for α-8T. The corresponding two SE lines emerge at respectively 553 nm and 512 nm for α-4T and 645 nm and 595 nm for α-6T. Gain narrowing of these two lines can be easily described in the usual framework of stimulated emission (SE). Light amplification originates from the combination of a net dipole alignment and efficient waveguiding towards the edges of the crystal. In contrast to dye-doped crystals like anthracene in a fluorene matrix,[192,193] the α-8T molecules and crystal provide both the emitter and the optical cavity respectively due to their quasi-2D dimensions.

Spectral SE selection of the two SE lines at 640 and 700 nm can be monitored by simply scanning the spatial position of the pump beam onto the surface of the α-8T crystal. The pump beam (energy = 4.0 μJ per pulse) is focused to a diameter of 0.3 mm and its position is scanned along the *x*-direction, *i.e.* the crystal length. As expected for this pump energy, the SE line at 700 nm dominates over most of the crystal surface while that at 640 nm is almost inactive (Fig. 18a). Fig. 18b shows that the situation is totally reversed in a small region located close to the crystal origin, the dominating SE line being that at 640 nm although residual activity of the line at 700 nm persists. These results suggest that spectral SE selection can be related either to a thickness effect or to the presence of structural defects whose inhomogeneous distribution could influence the emission process.

Two-photon SE can be easily realized in plane parallel single crystals of α-4T, α-6T and α-8T by pumping with a near-IR laser beam in-between the lower and upper faces of the crystal[189,190] (Fig. 19). Since the crystals are almost transparent in this region, it allows the pump beam to propagate through the crystal, thus "seeding" the up-converted SE beam on longer distances (Fig. 20). Excitation and up-converted detection are performed along the same direction perpendicular to the *a*-axis of the crystals. Under pumping in the 750–900 nm range, the two-photon excitation spectrum of a α-8T crystal peaks at

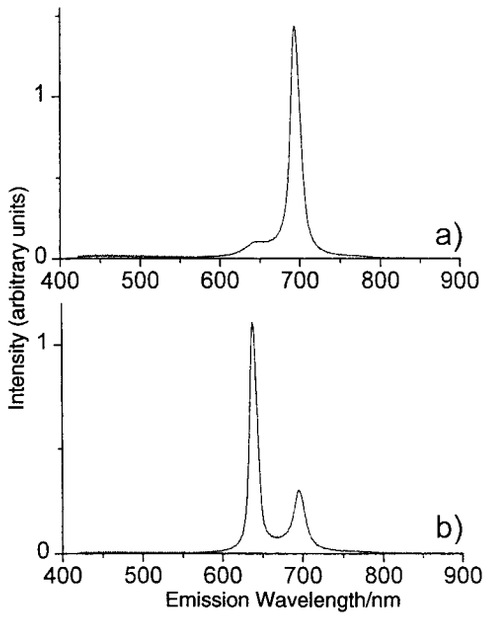

Fig. 18 Spatial dependence of stimulated emission in a α-8T single crystal when the pump beam (diameter = 0.3 mm) is scanned along the *x*-direction from the edge toward the inner part of the crystal. The two SE spectra shown here are recorded (a) in the outer and (b) in the inner regions of the crystal. Reproduced with permission from ref. 187.

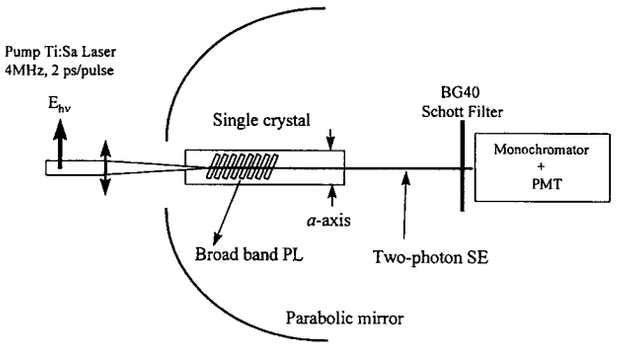

Fig. 19 Experimental setup for the observation of two-photon luminescence in α-*n*T single crystals. The near-IR pumping beam is directed parallel to the crystal plane (instead of normal) to increase the excitation length. Reprinted from *Synth. Met.*, 1999, **101**, 610, D, Fichon, V. Dumarcher and J.-M. Nunzi, Copyright (1999), with permission from Elsevier Science.

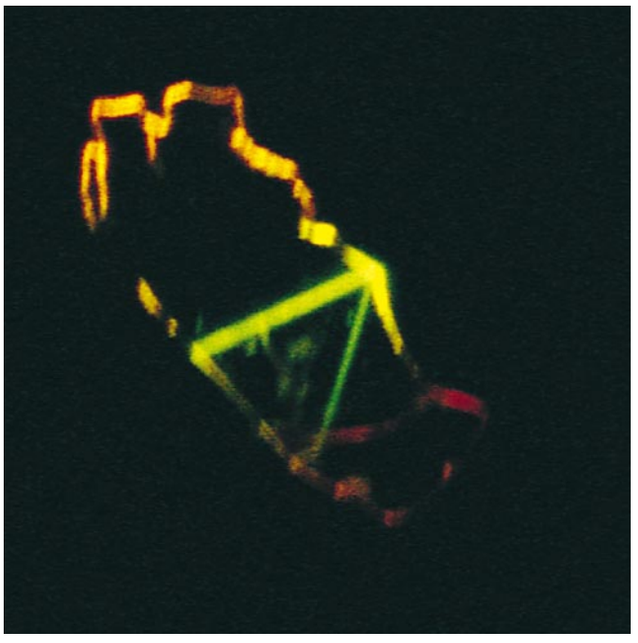

Fig. 20 Top view photograph of the intense and highly directional two-photon emission (yellow) in a α-4T single crystal (area = 7×4 mm^2). Note the presence of a reflected beam (green) of lower intensity inside the crystal. Reprinted from *Opt. Mater.*, 1999, **12**, 255, D. Fichou, V. Dumarcher and J.-M. Nunzi, Copyright (1999), with permission from Elsevier Science.

850 nm. Then, when an optical pump at 850 nm is used, the energy threshold for spectral narrowing in a α-8T crystal is estimated to be around 32 μJ cm^{-2}. Such an ultra-low up-converted SE threshold is the result of the particular gain-guiding geometry achieved in the strongly anisotropic crystal. Another important consequence of gain-guiding is the highly directive nature of the two-photon SE beam inside the crystal.

Since oligothiophenes are efficient organic semiconductors (with mobilities close to 0.1 cm^2 V^{-1} s^{-1}), one- and two-photon SE phenomena bridge the gap between conventional organic laser dyes and luminescent conjugated polymers on the way towards the organic laser diode.[194,195] The fabrication of such an organic laser diode requires a material combining efficient charge injection from the electrodes, good transport properties and reasonable luminescence efficiency in the solid state. This is obviously the case of α-6T and α-8T and laser diodes based on oligothiophenes thin films is currently under way. Finally, we should mention that very recently Gigli *et al.* reported on high efficiency LEDs (1.2 cd A^{-1}; turn-on voltages up to 1.9 V) based on "de-aromatized" oligothiophenes.[196] The

high solid state photoluminescence efficiency (up to 37%) of these unusual oligomers is attributed to structural order and opens a way for a new generation of organic LEDs.

4 Conclusion and outlook

The field of "polymer electronics" is very promising. In this context, we have shown that oligothiophenes are unique materials meeting the requirements of microelectronics and could find use in a number of devices. They can be obtained with high purity levels (electronic grade) and can be easily processed as ordered thin films or crystals with low-cost methods. 3D-supramolecular organization combined with extended π-systems is at the origin of their excellent transport properties. We note that in the course of this review, record hole mobilities of 0.9 and 10 $cm^2 V^{-1} s^{-1}$ have been measured by Schön *et al.* on α-6T crystals at respectively 300 and 4.2 K[197] while de Haas *et al.* were able to measure mobility of α-4T and α-6T oriented films by means of a microwave conductivity technique.[198,199]

Improvement and downscaling of organic devices requires to control the correlations between local topographic features and electronic properties at the nanometre scale. New approaches using near-field techniques like light-assisted STM[200] and conducting probe AFM[201,202] are currently developed on α-6T crystals and films. The first technique provides a through-space access to the local current-voltage characteristics of organic semiconductors. The {STM tip/air gap/α-6T} system simulates a photovoltaic nano-cell which can help unveil the intimate mechanisms of photocurrent generation.

Finally, more fundamental studies are still needed to understand the electronic properties of oligothiophenes. Since most organic devices utilize the excited states of the molecules it is important to control the extension of molecular excitons. Very recently, studies on oligothiophenes of various lengths (up to α-8T) and other well-defined π-conjugated systems led Knupfer *et al.* to establish a general rule for the exciton size.[203]

Acknowledgements

The author wishes to thank all the people who contributed to this work with a special mention to C. Videlot, A. Yassar, G. Horowitz, J.-M. Nunzi, F. Charra, C. Ziegler, A. Schoonveld, T. Klapwijk, J. Fink, M. Knupfer and M. P. de Haas for fruitful discussions. The author is also grateful to A. El Kassmi and S. Berteaux for the synthesis of 8T, to J.-L. Pastol for recording the SEM micrographs and to I. Billy and J. Thianche for the photographs of the single crystals.

References

1 *Handbook of Oligo- and Polythiophenes*, ed. D. Fichou, WILEY-VCH, Weinheim, 1999.
2 U. Schoeler, K. H. Tews and H. Kuhn, *J. Chem. Phys.*, 1974, **61**, 5009.
3 M. Akimoto, Y. Furukawa, H. Takeuchi, I. Harada, Y. Soma and M. Soma, *Synth. Met.*, 1986, **15**, 353.
4 Y. Yumoto and S. Yoshimura, *Synth. Met.*, 1986, **13**, 185.
5 S. Tasaka, H. E. Katz, R. S. Hutton, J. Orenstein, G. H. Fredrickson and T. T. Wang, *Synth. Met.*, 1986, **16**, 17.
6 J. Kagan and G. Chan, *Experientia*, 1983, **39**, 402.
7 J. B. Hudson, *Antiviral Res.*, 1989, **12**, 55.
8 R. Rossi, A. Carpita, M. Ciofalo and J. L. Houben, *Gazz. Chim. Ital.*, 1990, **120**, 793.
9 D. Fichou, G. Horowitz, Y. Nishikitani and F. Garnier, *Chemtronics*, 1988, **3**, 176.
10 G. Horowitz, D. Fichou and F. Garnier, *Solid State Commun.*, 1989, **70**, 385.
11 G. Horowitz, D. Fichou, X. Peng, Z. Xu and F. Garnier, *Solid State Commun.*, 1989, **72**, 381.
12 X. Peng, G. Horowitz, D. Fichou and F. Garnier, *Appl. Phys. Lett.*, 1990, **57**, 2013.
13 A. Tsumura, H. Koezuka and T. Ando, *Synth. Met.*, 1988, **25**, 11.
14 A. Assadi, C. Svensson, M. Wilander and O. Inganäs, *Appl. Phys. Lett.*, 1988, **53**, 195.
15 S. M. Sze, *Physics of Semiconductor Devices*, Wiley, New York, 1981.
16 F. Garnier, G. Horowitz, D. Fichou and X. Peng, *Adv. Mater.*, 1990, **2**, 592.
17 R. Zamboni, N. Periasamy, G. Ruani and C. Taliani, *Synth. Met.*, 1993, **54**, 57.
18 C. Taliani and L. M. Blinov, *Adv. Mater.*, 1996, **8**, 353.
19 D. Oeter, H.-J. Egelhaaf, Ch. Ziegler, D. Oelkrug and W. Göpel, *J. Chem. Phys.*, 1994, **101**, 6344.
20 For a review, see W. Gebauer and and C. Taliani, in *Handbook of Oligo- and Polythiophenes*, ed. D. Fichou, WILEY-VCH, Weinheim, 1999, pp. 361–404.
21 G. Horowitz, R. Hajlaoui and P. Delannoy, *J. Phys. III*, 1995, **5**, 355.
22 K. Waragai, H. Akamichi, S. Hotta, H. Kano and H. Sakaki, *Phys. Rev. B*, 1995, **52**, 1786.
23 L. Torsi, A. Dodabalapur, L. J. Rothberg, A. W. P. Fung and H. E. Katz, *Phys. Rev. B*, 1998, **57**, 2271.
24 For a review, see G. Horowitz and P. Delannoy, in *Handbook of Oligo- and Polythiophenes*, ed. D. Fichou, WILEY-VCH, Weinheim, 1999, pp. 283–316.
25 S. Hotta and K. Waragai, *Adv. Mater.*, 1993, **5**, 896.
26 F. Garnier, G. Horowitz, D. Fichou and A. Yassar, *Supramol. Sci.*, 1997, **4**, 155.
27 G. Horowitz, R. Hajlaoui and F. Kouki, *Eur. Phys. J: Appl. Phys.*, 1998, **1**, 361.
28 For a survey of oligothiophene TFTs, see H. E. Katz, A. Dodabalapur and Z. Bao, in *Handbook of Oligo- and Polythiophenes*, ed. D. Fichou, WILEY-VCH, Weinheim, 1999, pp. 459–489.
29 F. Geiger, M. Stoldt, H. Schweizer, P. Bäuerle and E. Umbach, *Adv. Mater.*, 1993, **5**, 922.
30 G. Horowitz, P. Delannoy, H. Bouchriha, F. Deloffre, J.-L. Fave, F. Garnier, R. Hajlaoui, M. Heyman, F. Kouki, P. Valat, V. Wintgens and A. Yassar, *Adv. Mater.*, 1994, **6**, 752.
31 D. Fichou, J.-M. Nunzi, F. Charra and N. Pfeffer, *Adv. Mater.*, 1994, **6**, 64.
32 F. Charra, M.-P. Lavie, A. Lorin and D. Fichou, *Synth. Met.*, 1994, **65**, 13.
33 M. G. Harrison, R. H. Friend, F. Garnier and A. Yassar, *Synth. Met.*, 1994, **67**, 215.
34 D. Fichou and F. Charra, *Synth. Met.*, 1996, **76**, 11.
35 N. Noma, T. Tsuzuki and Y. Shirota, *Adv. Mater.*, 1995, **7**, 647.
36 D. Fichou, F. Charra and A. Gusev, Material Research Society (MRS) Fall Meeting, Boston, USA, 1998.
37 C. Videlot and D. Fichou, *Synth. Met.*, 1999, **102**, 885.
38 C. Videlot, A. El Kassmi and D. Fichou, *Solar Energy Mater.*, in the press.
39 M. Granström, M. G. Harrison and R. H. Friend, in *Handbook of Oligo- and Polythiophenes*, ed. D. Fichou, WILEY-VCH, Weinheim, 1999, pp. 405–458.
40 Y. Delugeard, J. Desuche and J. L. Baudour, *Acta Crystallogr., Sect. B*, 1976, **32**, 702.
41 J. L. Baudour, H. Cailleau and W. B. Yelon Rivet, *Acta Crystallogr., Sect. B*, 1977, **33**, 1773.
42 J. L. Baudour, Y. Delugeard and P. Rivet, *Acta Crystallogr., Sect. B*, 1978, **33**, 625.
43 K. N. Baker, A. V. Fratini, T. Resch, H. C. Knachel, W. W. Adams, E. P. Socci and B. L. Farmer, *Polymer*, 1993, **34**, 1571.
44 S. Hotta and K. Waragai, *J. Mater. Chem.*, 1991, **1**, 835.
45 J.-H. Liao, M. Benz, E. LeGoff and M. G. Kanatzidis, *Adv. Mater.*, 1994, **6**, 135.
46 F. Van Bolhuis, H. Wynberg, E. E. Havinga, E. W. Meijer and E. G. J. Staring, *Synth. Met.*, 1989, **30**, 381.
47 A. Gavezzotti and G. Filippini, *Synth. Met.*, 1991, **40**, 257.
48 W. Porzio, S. Destri, M. Mascherpa and S. Brückner, *Acta Polym.*, 1993, **44**, 266.
49 P. Ostoja, S. Guerri, S. Rossini, M. Servidori, C. Taliani and R. Zamboni, *Synth. Met.*, 1993, **54**, 447.
50 B. Servet, S. Ries, M. Trotel, P. Alnot, G. Horowitz and F. Garnier, *Adv. Mater.*, 1993, **5**, 461.
51 B. Servet, G. Horowitz, S. Ries, O. Lagorsse, P. Alnot, A. Yassar, F. Deloffre, P. Srivastava, R. Hajlaoui, P. Lang and F. Garnier, *Chem. Mater.*, 1994, **6**, 1809.

52 Y. Kanemitsu, N. Shimizu, K. Suzuki, Y. Shiraishi and M. Kuroda, *Phys. Rev. B*, 1996, **54**, 2198.
53 G. J. Visser, G. J. Heeres, J. Wolters and A. Vos, *Acta Crystallogr., Sect. B*, 1968, **24**, 467.
54 P. A. Chaloner, S. R. Gunatunga and P. B. Hitchcock, *Acta Crystallogr., Sect. C*, 1994, **50**, 1941.
55 M. Pelletier and F. Brisse, *Acta Crystallogr., Sect. C*, 1994, **50**, 1942.
56 L. Antolini, G. Horowitz, F. Kouki and F. Garnier, *Adv. Mater.*, 1998, **10**, 382.
57 T. Siegrist, Ch. Kloc, R. A. Laudise, H. E. Katz and R. C. Haddon, *Adv. Mater.*, 1998, **10**, 379.
58 W. Porzio, S. Destri, M. Mascherpa, S. Rossini and S. Brückner, *Synth. Met.*, 1993, **55**, 408.
59 G. Horowitz, B. Bachet, A. Yassar, P. Lang, F. Demanze, J. L. Fave and F. Garnier, *Chem. Mater.*, 1995, **7**, 1337.
60 D. Fichou, B. Bachet, F. Demanze, I. Billy, G. Horowitz and F. Garnier, *Adv. Mater.*, 1996, **6**, 500.
61 T. Siegrist, R. M. Fleming, R. C. Haddon, R. A. Laudise, A. J. Lovinger, H. E. Katz, P. Bridenbaugh and D. D. Davis, *J. Mater. Res.*, 1995, **10**, 2170.
62 Z. Mo, K.-B. Lee, Y. B. Moon, M. Kobayashi, A. J. Heeger and F. Wudl, *Macromolecules*, 1985, **18**, 1972.
63 C. X. Cui and M. Kertesz, *Phys. Rev. B*, 1989, **40**, 9661.
64 D. R. Ferro, W. Porzio, S. Destri, M. Ragazzi and S. Brückner, *Macromol. Theory Simul.*, 1997, **6**, 713.
65 Y. Matsuura, Y. Oshima, Y. Misaki, H. Fujiwara, K. Tanaka, T. Yamabe and S. Hotta, *Synth. Met.*, 1996, **82**, 155.
66 G. Barbarella, M. Zambianchi, A. Bongini and L. Antonili, *Adv. Mater.*, 1992, **4**, 282.
67 G. Barbarella, A. Bongini and M. Zambianchi, *Adv. Mater.*, 1991, **3**, 494.
68 G. Barbarella, M. Zambianchi, R. Di Toro, M. Colonna, L. Antolini and A. Bongini, *Adv. Mater.*, 1996, **8**, 327.
69 G. Barbarella, M. Zambianchi, M. del Fresno I. Marimon, L. Antolini and A. Bongini, *Adv. Mater.*, 1997, **9**, 484.
70 J. Bernstein and A. T. Hagler, *J. Am. Chem. Soc.*, 1978, **100**, 673.
71 J. D. Dunitz and J. Bernstein, *Acc. Chem. Res.*, 1995, **28**, 193.
72 C. Taliani, R. Zamboni, G. Ruani, S. Rossini and R. Lazzaroni, *J. Mol. Electron.*, 1990, **6**, 225.
73 S. Destri, M. Mascherpa and W. Porzio, *Adv. Mater.*, 1993, **5**, 43.
74 F. R. Lipsett, *Can. J. Phys.*, 1957, **35**, 284.
75 J. H. Schön, Ch. Kloc, R. A. Laudise and B. Batlogg, *Phys. Rev. B*, 1998, **58**, 12952.
76 R. A. Laudise, P. M. Bridenbaugh, T. Siegrist, R. M. Fleming, H. E. Katz and A. J. Lovinger, *J. Cryst. Growth*, 1995, **152**, 241.
77 J. K. Herrema, J. Wilderman, F. Van Bolhuis and G. Hadziioannou, *Synth. Met.*, 1993, **60**, 239.
78 F. Garnier, A. Yassar, R. Hajaloui, F. Deloffre, B. Servet, S. Ries and P. Alnot, *J. Am. Chem. Soc.*, 1993, **115**, 8716.
79 G. Barbarella, P. Ostoja, P. Maccagnani, O. Pudova, L. Antolini, D. Casarini and A. Bongini, *Chem. Mater.*, 1998, **10**, 3683.
80 A. Yassar, F. Garnier, F. Deloffre, G. Horowitz and L. Ricard, *Adv. Mater.*, 1994, **6**, 660.
81 T. M. Barclay, A. W. Cordes, C. D. MacKinnon, R. T. Oakley and R. W. Reed, *Chem. Mater.*, 1997, **9**, 981.
82 D. Fichou, M.-P. Teulade-Fichou, G. Horowitz and F. Demanze, *Adv. Mater.*, 1997, **9**, 75.
83 R. Hajlaoui, D. Fichou, G. Horowitz, B. Nessakh, M. Constant and F. Garnier, *Adv. Mater.*, 1997, **9**, 557.
84 D. Fichou, F. Garnier, F. Charra, F. Kajzar and J. Messier, *Organic Materials for Nonlinear Optics*, eds. R. Hahn and D. Bloor, Royal Society of Chemistry, London, 1989, p. 176.
85 C. Videlot, A. Yassar, D. Fichou, T. Isoshima, T. Wada and H. Sasabe, *Mol. Cryst. Liq. Cryst.*, 1998, **322**, 29.
86 H. Knobloch, D. Fichou, W. Knoll and H. Sasabe, *Adv. Mater.*, 1993, **5**, 570.
87 F. Garnier, G. Tourillon, J. Y. Barraud and H. Dexpert, *J. Mater. Sci.*, 1985, **20**, 2687.
88 R. Yang, K. M. Dalsin, D. F. Evans, L. Christensen and W. A. Hendrickson, *J. Phys. Chem.*, 1989, **65**, 23.
89 J.-P. Aime, F. Bargain, M. Schott, H. Eckhardt, G. G. Miller and R. L. Elsenbaumer, *Phys. Rev. Lett.*, 1989, **62**, 55.
90 O. Inganäs, W. R. Salaneck, J. E. Osterholm and J. Laasko, *Synth. Met.*, 1988, **22**, 395.
91 W. R. Salaneck, O. Inganäs, B. Theman, J. O. Nilson, B. Sjogren, J. E. Osterholm, J.-L. Brédas and S. Svensson, *J. Chem. Phys.*, 1988, **89**, 4613.
92 S. Bruckner and W. Porzio, *Makromol. Chem.*, 1988, **189**, 961.
93 M. J. Winokur, D. Spiegel, Y. Kim, S. Hotta and A. J. Heeger, *Synth. Met.*, 1989, **28**, C419.
94 T. Yamamoto, T. Kanbara and C. Mori, *Synth. Met.*, 1990, **38**, 399.
95 J. Mardalen, E. J. Samuelsen, O. R. Gautun and P. H. Carlsen, *Synth. Met.*, 1992, **48**, 363.
96 C. Ziegler, in *Handbook of Organic Conductive Molecules and Polymers*, ed. H. S. Nalwa, John Wiley and Sons Ltd., New York, Vol. 3, 1997, p. 677.
97 D. Fichou and C. Ziegler, in *Handbook of Oligo- and Polythiophenes*, ed. D. Fichou, WILEY-VCH, Weinheim, 1999, p. 183.
98 F. Biscarini, R. Zamboni, P. Samori, P. Ostoja and C. Taliani, *Phys. Rev. B*, 1995, **52**, 14868.
99 A. J. Lovinger, H. E. Katz and A. Dodabalapur, *Chem. Mater.*, 1998, **10**, 3275.
100 J. G. Laquindanum, H. E. Katz and A. J. Lovinger, *J. Am. Chem. Soc.*, 1998, **120**, 664.
101 A. Soukopp, C. Seidel, R. Li, M. Bässler, M. Skolowski and E. Umbach, *Thin Solid Films*, 1996, **284–285**, 343.
102 A. Soukopp, K. Glöker, P. Kraft, S. Schmitt, M. Sokolowski, E. Umbach, E. Mena-Osteritz, P. Bäuerle and E. Hädicke, *Phys. Rev. B*, 1998, **58**, 13882.
103 N. B. Nardelli, D. Cvetko, V. De Renzi, L. Floreano, R. Gouter, A. Morgante, M. Peloi, F. Tommasini, R. Danielli, S. Rossini, C. Taliani and R. Zamboni, *Phys. Rev. B*, 1995, **53**, 1095.
104 C. Ludwig, B. Gompf, J. Petersen, R. Strohmaier and W. Eisenmenger, *Z. Phys. B*, 1994, **240**, 127.
105 D. Oelkrug, H.-J. Egelhaaf and J. Haiber, *Thin Solid Films*, 1996, **284–285**, 267.
106 A. Borghesi, A. Sassella, R. Tubino, S. Destri and W. Porzio, *Adv. Mater.*, 1998, **10**, 931.
107 N. S. Sariciftci, U. Lemmer, D. Vacar, A. J. Heeger and R. A. J. Janssen, *Synth. Met.*, 1997, **84**, 609.
108 J. V. Caspar, V. Ramamurthy and D. R. Corbin, *J. Am. Chem. Soc.*, 1991, **113**, 600.
109 P. Enzel and T. Bein, *Synth. Met.*, 1993, **55–57**, 1238.
110 Y. Y. Lin, D. J. Gundlach and T. N. Jackson, *IEEE Trans. Electron Devices*, 1997, **44**, 8.
111 S. F. Nelson, Y. Y. Lin, D. J. Gundlach and T. N. Jackson, *Appl. Phys. Lett.*, 1998, **72**, 1854.
112 G. Horowitz, F. Garnier, A. Yassar, R. Hajlaoui and F. Kouki, *Adv. Mater.*, 1996, **8**, 52.
113 H. E. Katz, *J. Mater. Chem.*, 1997, **7**, 369.
114 G. Horowitz, R. Hajlaoui, D. Fichou and A. El Kassmi, *J. Appl. Phys.*, 1999, **85**, 3202.
115 G. Horowitz, X. Z. Peng, D. Fichou and F. Garnier, *J. Mol. Electron.*, 1991, **7**, 85.
116 H. Akimichi, K. Waragai, S. Hotta, H. Kano and H. Sakaki, *Appl. Phys. Lett.*, 1991, **58**, 1500.
117 H. E. Katz, L. Torsi and A. Dodabalapur, *Chem. Mater.*, 1995, **7**, 2235.
118 R. Hajlaoui, G. Horowitz, F. Garnier, A. Arce-Brouchet, L. Laigre, A. El Kassmi, F. Demanze and F. Kouki, *Adv. Mater.*, 1997, **9**, 389.
119 H. E. Katz, A. J. Lovinger and J. G. Laquindanum, *Chem. Mater.*, 1998, **10**, 457.
120 F. Ebisawa, T. Kurokawa and S. Nara, *J. Appl. Phys.*, 1983, **54**, 3255.
121 Z. Bao, A. J. Lovinger and A. Dodabalapur, *Appl. Phys. Lett.*, 1996, **69**, 4108.
122 H. Sirringhaus, N. Tessler and R. H. Friend, *Science*, 1998, **280**, 1741.
123 R. Hajlaoui, D. Fichou, A. Yassar and G. Horowitz, unpublished work.
124 J. H. Schön, Ch. Kloc, R. A. Laudise and B. Batlogg, *Appl. Phys. Lett.*, 1998, **73**, 3574.
125 W. A. Schoonveld, R. W. Stok, J. W. Weijtmans, J. Vrijmoeth, J. Wildeman and T. M. Klapwijk, *Synth. Met.*, 1997, **84**, 583.
126 W. A. Schoonveld, J. Vrijmoeth and T. M. Klapwijk, *Appl. Phys. Lett.*, 1998, **73**, 3884.
127 W. A. Schoonveld, J. Wildeman, D. Fichou, P. A. Bobbert, B. J. van Wees and T. M. Klapwijk, submitted to *Nature*.
128 J. Vrijmoeth, R. W. Stok, R. Veldman, W. A. Schoonveld and T. M. Klapwijk, *J. Appl. Phys.*, 1998, **83**, 3816.
129 G. Barbarella, P. Ostoja, P. Maccagnani, O. Pudova, L. Antoilini, D. Casarini and A. Bongini, *Chem. Mater.*, 1998, **10**, 3683.
130 H. Sirringhaus, R. H. Friend, C. Wang, J. Leuninger and K. Müllen, *J. Mater. Chem.*, 1999, **9**, 2095.
131 R. D. McCullough and R. D. Lowe, *J. Chem. Soc., Chem. Commun.*, 1992, 70.
132 R. D. McCullough, in *Handbook of Oligo- and Polythiophenes*, ed. D. Fichou, WILEY-VCH, Weinheim, 1999, pp. 1–44.

133 Z. Bao, Y. Feng, A. Dodabalapur, V. R. Raju and A. J. Lovinger, *Chem. Mater.*, 1997, **9**, 1299.
134 I. D. Parker, R. W. Gymer, M. G. Harisson, R. H. Friend and H. Ahmed, *Appl. Phys. Lett.*, 1993, **62**, 1519.
135 T. Kurata, C. Fukada, H. Fuchigami, K. Hamano and S. Tsunoda, *Thin Solid Films*, 1998, **331**, 55.
136 P. M. Borsenberger and D. S. Weiss, *Organic Receptors for Imaging Systems*, ed. B. J. Thompson, Marcel Dekker, Inc., New York, 1993, vol. 39.
137 O. Dippel, V. Brandl, H. Bässler, R. Danieli, R. Zamboni and C. Taliani, *Chem. Phys. Lett.*, 1993, **216**, 418.
138 R. Zamboni, N. Periasamy, G. Ruani and C. Taliani, *Synth. Met.*, 1993, **54**, 57.
139 G. Horowitz, S. Romdhane, H. Bouchriha, P. Delannoy, J.-L. Monge, F. Kouki and P. Valat, *Synth. Met.*, 1997, **90**, 187.
140 D. Moses, J. Wang, A. Dogariu, D. Fichou and C. Videlot, *Phys. Rev. B*, 1999, **59**, 7715.
141 C. W. Tang, *Appl. Phys. Lett.*, 1986, **48**, 183.
142 D. Wöhrle and D. Meissner, *Adv. Mater.*, 1991, **3**, 129.
143 M. Hiramoto, H. Fujiwara and M. Yokoyama, *J. Appl. Phys.*, 1992, **72**, 3781.
144 J. B. Whitlock, P. Panayotatos, G. D. Sharma, M. D. Cox, R. R. Sauers and G. R. Bird, *Opt. Eng.*, 1993, **32**, 1921.
145 H. Yanagi, N. Tamura, S. Taira, H. Furuta, S. Douko, G. Schnurpfeil and D. Wöhrle, *Mol. Cryst. Liq. Cryst.*, 1995, **267**, 435.
146 T. Tsuzuki, N. Hirota, N. Noma and Y. Shirota, *Thin Solid Films*, 1996, **273**, 177.
147 R. N. Marks, J. J. Halls, D. D. C. Bradley, R. H. Friend and A. B. Holmes, *J. Phys.: Condens. Mater.*, 1994, **6**, 1379.
148 H. Antoniadis, B. R. Hsieh, M. A. Abkowitz, S. A. Jenekhe and M. Stolka, *Synth. Met.*, 1994, **62**, 265.
149 G. Yu, C. Zhang and A. J. Heeger, *Appl. Phys. Lett.*, 1994, **64**, 1540.
150 J. J. M. Halls, K. Pichler, R. H. Friend, S. C. Moratti and A. B. Holmes, *Appl. Phys. Lett.*, 1996, **68**, 3120.
151 D. Adam, P. Schumacher, J. Simmerer, L. Haussling, K. Siemensmeyer, K. Etzbach, H. Ringsdorf and D. Haarer, *Nature*, 1994, **371**, 141.
152 J. Gao, G. Yu and A. J. Heeger, *Adv. Mater.*, 1998, **10**, 692.
153 G. Yu, J. Gao, J. C. Hummelen, F. Wudl and A. J. Heeger, *Science*, 1995, **270**, 1789.
154 G. Horowitz and F. Garnier, *Solar Energy Mater.*, 1986, **13**, 47.
155 Y. Fang, S.-A. Chen and M. L. Chu, *Synth. Met.*, 1992, **52**, 261.
156 C. Sène, H. Nguyen Cong and P. Chartier, *Solar Energy Mater.*, 1997, **52**, 413.
157 R. N. Marks, R. Zamboni and C. Taliani, MRS Fall Meeting, Boston, 1995.
158 K. Yoshino, X. H. Yin, S. Morita, T. Kawai and A. A. Zakhidov, *Solid State Commun.*, 1993, **85**, 85.
159 L. S. L. Roman, M. R. Andersson, T. Yohannes and O. Inganäs, *Adv. Mater.*, 1997, **9**, 1164.
160 N. S. Sariciftci and A. J. Heeger, *Int. J. Mod. Phys. B*, 1994, **8**, 237.
161 N. S. Sariciftci, L. Smilowitz, A. J. Heeger and F. Wudl, *Science*, 1992, **258**, 1474.
162 M. Granström, K. Petrisch, A. C. Arias, A. Lux, M. R. Andersson and R. H. Friend, *Nature*, 1998, **395**, 257.
163 H.-J. Egelhaaf and D. Oelkrug, *SPIE Proc.*, 1995, **2362**, 398.
164 D. Oelkrug, H.-J. Egelhaaf, D. R. Worrall and F. Wilkinson, *J. Fluoresc.*, 1995, **5**, 165.
165 F. Deloffre, F. Garnier, P. Srivastava, A. Yassar and J.-L. Fave, *Synth. Met.*, 1994, **67**, 23.
166 A. Yassar, G. Horowitz, P. Valat, V. Wintgens, M. Hmyene, F. Deloffre, P. Srivastava, P. Lang and F. Garnier, *J. Phys. Chem.*, 1995, **99**, 9155.
167 H-J. Egelhaaf, D. Oelkrug, D. Oeter, C. Ziegler and W. Göpel, *J. Mol. Struct. (THEOCHEM)*, 1995, **348**, 405.
168 K. Hamano, T. Kurata, S. Kubota and H. Koezuka, *Jpn. J. Appl. Phys.*, 1994, **33**, L1031.
169 M. Muccini, E. Lunedei, A. Bree, G. Horowitz, F. Garnier and C. Taliani, *J. Chem. Phys.*, 1998, **108**, 7327.
170 D. Oelkrug, H.-J. Egelhaaf and J. Haiber, *Thin Solid Films*, 1996, **284**, 267.
171 K. Uchiyama, H. Akimichi, S. Hotta, H. Noge and H. Sakaki, *Synth. Met.*, 1994, **63**, 57.
172 C. Väterlein, H. Neureiter, W. Gebauer, B. Ziegler, M. Sokolowski, P. Bäuerle and E. Umbach, *J. Appl. Phys.*, 1997, **82**, 3003.
173 F. Cacialli, R. N. Marks, R. H. Friend, R. Zamboni, C. Taliani, S. C. Moratti and A. B. Holmes, *Synth. Met.*, 1996, **76**, 145.
174 T. Noda, H. Ogawa, N. Noma and Y. Shirota, *Appl. Phys. Lett.*, 1997, **70**, 699.
175 T. Noda and Y. Shirota, *J. Am. Chem. Soc.*, 1998, **120**, 9714.
176 Y. Ohmori, M. Uchida, K. Muro and K. Yoshino, *Solid State Commun.*, 1991, **80**, 605.
177 D. Braun, G. Gustafsson, D. McBranch and A. J. Heeger, *J. Appl. Phys.*, 1992, **72**, 564.
178 N. C. Greenham, A. R. Brown, D. D. C. Braddley and R. H. Friend, *Synth. Met.*, 1993, **55–57**, 4134.
179 F. Chen, P. C. Mehta, L. Takiff and R. D. McCullough, *J. Mater. Chem.*, 1996, **6**, 1763.
180 R. Gill, G. C. Malliaras, J. Wildeman and G. Hadziioannou, *Adv. Mater.*, 1994, **6**, 132.
181 P. Barta, F. Cacialli, R. H. Friend and M. Zagorska, *J. Appl. Phys.*, 1998, **84**, 6279.
182 R. N. Marks, F. Biscarini, T. Virgili, M. Muccini, R. Zamboni and C. Taliani, *Philos. Trans. R. Soc. London A.*, 1997, **355**, 763.
183 R. N. Marks, F. Biscarini, R. Zamboni and C. Taliani, *Europhys. Lett.*, 1995, **32**, 523.
184 P. Dyreklev, M. Berggren, O. Inganäs, M. R. Andersson, O. Wennerström and T. Hjertberg, *Adv. Mater.*, 1995, **7**, 43.
185 A. Bolognesi, G. Bajo, J. Paloheimo, T. Östergard and H. Stubb, *Adv. Mater.*, 1997, **9**, 121.
186 T. Granlund, M. Theander, M. Berggren, M. Andersson, A. Ruzeckas, V. Sundström, G. Björk, M. Granström and O. Inganäs, *Chem. Phys. Lett.*, 1998, **288**, 879.
187 D. Fichou, S. Delysse and J.-M. Nunzi, *Adv. Mater.*, 1997, **9**, 1178.
188 G. Horowitz, P. Valat, F. Garnier, F. Kouki and V. Wintgens, *Opt. Mater.*, 1998, **9**, 46.
189 D. Fichou, V. Dumarcher, S. Delysse and J.-M. Nunzi, Proceedings of the SPIE Conference, San Jose, USA, 1998.
190 (*a*) D. Fichou, V. Dumarcher and J.-M. Nunzi, *Opt. Mater.*, 1999, **12**, 255; (*b*) D. Fichou, V. Dumarcher and J.-M. Nunzi, *Synth. Met.*, 1999, **101**, 610.
191 G. Horowitz, F. Kouki, A. El Kassmi, P. Valat, V. Wintgens and F. Garnier, *Adv. Mater.*, 1999, **11**, 234.
192 N. Karl, *Phys. Status Solidi*, 1972, **13**, 651.
193 N. Karl, *J. Lumin.*, 1976, **12/13**, 851.
194 N. Tessler, G. J. Denton and R. H. Friend, *Nature*, 1996, **382**, 695.
195 F. Hide, M. A. Diaz-Garcia, B. J. Schwartz, M. R. Anderson, Q. Pei and A. J. Heeger, *Science*, 1996, **273**, 1833.
196 G. Gigli, G. Barbarella, L. Favaretto, F. Cacialli and R. Cingolani, *Appl. Phys. Lett.*, 1999, **75**, 439.
197 J. H. Schön, Ch. Kloc and B. Batlogg, 5th European Conference on Molecular Electronics (ECME'99), Linköping, Sweden, September 1999.
198 M. P. de Haas, G. P. van der Laan, B. Wegewijs, D. M. de Leeuw, P. Bauerle, D. B. A. Rep and D. Fichou, *Synth. Met.*, 1999, **101**, 524.
199 B. Wegewijs, M. P. de Haas, D. M. de Leeuw, R. Wilson and H. Sirringhaus, *Synth. Met.*, 1999, **101**, 534.
200 D. Fichou, F. Charra, A. Gusev and S. Quemener, 5th European Conference on Molecular Electronics (ECME'99), Linköping, Sweden, September 1999.
201 M. J. Loiacono, E. L. Granstrom and C. D. Frisbie, *J. Phys. Chem. B*, 1998, **102**, 1679.
202 T. W. Kelley, E. L. Granstrom and C. D. Frisbie, *Adv. Mater.*, 1999, **11**, 261.
203 M. Knupfer, J. Fink, E. Zojer, G. Leising and D. Fichou, submitted to *Chem. Phys. Lett*.

Paper a908312j